Available online at www.CivileJournal.org

Civil Engineering Journal

(E-ISSN: 2476-3055; ISSN: 2676-6957)

Vol. 10, No. 11, November, 2024

Study of Reversible Nozzle Apparatuses Using Euler Methodology and CFD Technologies

Yuri A. Sazonov [1], Mikhail A. Mokhov [1*], Anton V. Bondarenko [1], Victoria V. Voronova [1], Khoren A. Tumanyan [1], Egor I. Konyushkov [1]

[1] *National University of Oil and Gas, Gubkin University, Moscow, Russian Federation.*

Received 20 August 2024; Revised 21 October 2024; Accepted 26 October 2024; Published 01 November 2024

Abstract

This research aims to study multiflow nozzle apparatuses designed to control the thrust vector within a full geometric sphere when the deflection angle of the thrust vector can vary in the range from +180 °to -180 °in any direction. The distribution of the working gas energy was considered as exemplified by a reversible nozzle apparatus with two outlet channels. It was shown that when using wedge-shaped diaphragms, the critical section area can be regulated while maintaining a constant pressure and flow rate of the working gas entering the inlet of the multiflow nozzle. In this case, the mass flow rate of the gas and jet thrust in each outlet channel change in direct proportion to the linear displacement of the diaphragm. Known conical diaphragms do not provide these results. To create promising control systems and train designers, it is proposed to use the Euler methodology and CFD technologies more widely based on the philosophy of technology. In the course of the numerical experiments, the options for the thrust cutoff (tailoff) were considered. A scientific basis has been prepared for solving problems with six degrees of freedom in three-dimensional space, considering Euler angles, when controlling the thrust vector within a full geometric sphere. Issues in flight trajectory planning (for example, for an unmanned aerial vehicle) are discussed with regard to new possibilities for extreme maneuvering. Two main areas for the development of scientific research are considered: energy-saving power generation and transportation systems (land, sea, and air).

Keywords: Nozzle Apparatus; Thrust Vector; CFD-Technologies; Euler Methodology; Philosophy of Technology.

1. Introduction

Ejector systems are widely used in many industries, including power engineering [1, 2] and aerospace [3]. In most cases, the priority areas for the development of science, technology, and education today include highly efficient and environmentally friendly power engineering, with the appropriate adaptation of technologies to climate change with the active use of artificial intelligence. Furthermore, pivotal science-intensive technologies include transportation for various applications (land, sea, and air). Technologies related to the use of unmanned and autonomous robotic systems have particularly been highlighted. Many scientific and technical problems have been solved through interdisciplinary studies. The volume of information is rapidly increasing, and, under such conditions, the use of artificial intelligence tools is becoming inevitable. This article continues a series of publications [4-7] devoted to the issues of studying and practical use of complex ejector systems. A new scientific direction has emerged in the study of multiflow ejectors designed to control the thrust vector within a full geometric sphere when the thrust-vector deflection angle can range from +180° to -180° in any direction. In the context of applied scientific research, these publications [4-7] suggest the

* Corresponding author: mikhal.mokhov@mail.ru

http://dx.doi.org/10.28991/CEJ-2024-010-11-013

creation of extremely maneuverable high-speed transport systems (including unmanned systems) for operation on land, at sea, and in the air. New capabilities for controlling high-density energy flows will improve the efficiency of power engineering, mining, and mineral processing (including liquid and gaseous hydrocarbons). In the context of fundamental scientific research, these publications [4-7] are aimed at further studying the Euler methodology to find promising paths for the development of science and technology in the era of computerization and artificial intelligence. In the context of applied scientific studies and practical developments, the present article sets a specific goal to study the options for a multiflow nozzle apparatus designed to operate as a part of a multiflow ejector. Simple and inexpensive design solutions can also be applied to complex technologies, including aviation technology.

The design and manufacturing of industrial products are distinct areas of human social activity. The scientific field is the production of ideal objects, scientific knowledge, and knowledge systems. Education and upbringing are figuratively presented as a kind of production and "manufacturing" of people [8]. At the same time, the main factors that determine the division of labor in groups of specialists are usually the following two factors: 1) the time and pace of production of the product, that is, maximum productivity; and 2) the ability of one person to assimilate different knowledge. The second factor today is to slow the development of the system, and the system itself begins to react to this by actively introducing robotics and artificial intelligence into life. Detailing (specialization) in any system (and in a subsystem) can continue almost indefinitely, and this detailing will stop only at the level set by the goals of the study [8]. Rene Descartes noted the "rule of logic" in his study [9]: one should "divide each of the difficulties I consider into as many parts as necessary to better resolve them." It is known that Euler, in the particular case of describing a blade wheel, assumed an infinitely large number of blades with an infinitely small wall thickness for each blade. The Euler idea can be applied to a more general case [4-7]. In such a general case, an idealized mathematical model can contain an infinitely large number of parameters x_{ji}. The number of parameters increases as knowledge accumulates, and the mathematical model becomes more complex and strives for its ideal or perfection (theoretically unattainable perfection). When solving any optimization problem, the optimization criterion y can be represented as a certain function f depending on a set of parameters [4-7]:

$$y = f\left(x_{ji};\ x_{j(i+1)};\ x_{j(i+2)} \dots x_{jz} \dots x_{j\infty}\right) \tag{1}$$

In this case, according to Euler methodology, each parameter can be represented as follows:

$$x_{ji} = var \tag{2}$$

$$0 \le i \le \infty \tag{3}$$

According to Euler (Equations 1 to 3), the mathematical model includes four groups of indexed parameters [1-4], which correspond to four subgroups of parameters: indices (a, b, c, d) for the corresponding parameters $(x_{ai};\ x_{bi};\ x_{ci};\ x_{di})$. Index (a) represents the parameters that characterize the properties of the structural materials. Index (b) shows the geometric parameters that characterize the shape and dimensions of the product. The index (c) represents the gas-dynamic parameters that characterize the gas-dynamic processes in the flow channels. Index (d) represents the economic parameters that characterize the efficiency of the production process and the use of the product.

Considering the power of modern computers and the ambitions of artificial intelligence, such multiparameter problems with multidimensional spaces no longer frighten specialists, and possible restrictions are formulated very vaguely (for example, a scientific or technical result must be obtained by spending "reasonable" money in a "reasonable" time). Karl Raimund Popper noted that knowledge can grow and science can progress precisely because we are able to learn from our mistakes [10]. Since we learn from our mistakes, our knowledge grows, although we know nothing with complete certainty. In practice, science operates under the following assumptions: a leap to conclusions is possible even after a single observation [10].

Euler's mathematical model (formulas 1-3) allows for the development of a special theory for solving scientific and inventive problems. First, it is assumed that this Euler methodology is used to study the processes of interaction of a fluid with a solid wall [4-7], for example, a gas, liquid, or gas-liquid mixture can act as a fluid. Studying the process of fluid interaction with a solid wall is associated with solving multiparameter problems, which, in turn, form sets of multidimensional spaces (in terms of mathematics). This research has transformed into interdisciplinary research. Popper [10] drew attention to the fact that we study problems rather than objects, but that problems can cross the boundaries of any discipline and their objects. Some problems have remained relevant for many years. A challenging task is to fly further while saving fuel. Other tasks include reducing the radar visibility, noise, and infrared radiation [11]. The results can be obtained by optimizing the shape of the aircraft, including the shape of the fuselage and wing morphing [12]. Multidisciplinary optimization involves the development of hybrid power plants [13-15]. However, the known multidisciplinary studies weakly touch upon the theory of inventive and engineering work, without which it is difficult to imagine the active development of science and technology in the era of artificial intelligence.

It was decided to analyze scientific and technical information with regard to the well-known technology of big data merging – Multi-Source Information Fusion (MSIF) coming from many disparate sources [16], preferably in the field of aerospace technologies. These preferences are determined as follows: aerospace technologies have accumulated almost all the advanced achievements of science and technology in general (these are multidisciplinary scientific and technical developments). Aerospace technologies more vividly reflect the level of competition in the economy (the famous military doctrine of the Italian General Douhet about "superiority in the air" in a century becomes more and more relevant and more acute, gradually capturing all areas of people's lives). Aerospace technologies (after solving military problems) are actively used in the civilian economy and, almost always, are "unlimitedly" financed. Such a stable and effective source of new scientific and technical information, such as aerospace technology, objectively characterizes the level of development of science and technology in general in the present period.

With the active development of UAVs, new tasks have appeared to organize joint work for many unmanned vehicles, with the planning of many trajectories of movement and excluding collisions with obstacles or other aircraft [17-19]. There are restrictions on the choice of curvilinear trajectory for a fixed-wing UAV. The trajectory curvature is limited. It aims to achieve a balance between computational complexity and trajectory optimization for a UAV swarm designated as an unmanned aircraft system [20-22]. Complex problems have been solved for planning routes without UAV collisions [23-25], including the formation of UAV swarm [26-28]. Modular UAVs are currently being actively considered and studied [29]. One or more unmanned vehicles can interact with fixed-wing unmanned aircraft in the case of flexible connections [30, 31]. The flow of liquids and gases in tortuous channels (in "S"-shaped channels) is actively studied [4-6, 32]. When a rocket engine is turned off, the drag force increases significantly owing to the decrease in the pressure in the aft part of the rocket [33]. Both passive and active devices (units) that control the flow and move vortices downstream, achieving a decrease in base drag, have been studied in rocket and aviation engineering [34-36]. Computer modeling and forecasting of aerodynamics at high angles of attack (up to 80 °) are of great importance for the design and development of promising aircraft [37]. Reusable rockets rely on well-designed control algorithms [38]. The thrust of a rocket engine can be regulated in the following ways: by changing the critical section area, introducing an additional mass of the working fluid into the combustion chamber, changing the combustion surface, directly influencing the combustion rate, and thrust tailoff [39-41]. Research continues on various options for rocket engines, including hybrid and detonation rocket engines [42-44]. At the same time, the scientific and technical literature poorly describes the technical capabilities for multiple tailoffs (cutoff) of thrust while maintaining unchanged operating modes at the source of the working gas (or liquid). Options for using the energy of high-altitude jet streams in Earth's atmosphere are also considered [45]. Artificial intelligence technologies have been used to control unmanned vehicles [46-48]. Conceptual design technologies for aerospace engineering have also emerged [49, 50]. Increasing attention has been paid to increasing the speed and maneuverability of aircraft [51-53]. Within the framework of the international patent classification, new technical solutions (unmanned vehicles) are patented by classes: "B64U50/15" – propulsion systems using gas emissions from fuel combustion, for example, using rocket engines, "B64U50/18" – propulsion systems with thrust vector control.

Economic competition has accelerated the development of these technologies. According to early ideas, compete means to achieve suppression or takeover of rivals rather than compete with them in the market on equal terms [54, 55]. The periods of competition associated with mass production and demand are left behind. The habitual world of marketing and production has been replaced by an unusual world of unknown technologies, unexpected competitors, and new consumer demands [56]. In modern conditions, when competition covers all spheres of people's lives (science, technology, and education) with the connection of the growing forces of artificial intelligence, it is proposed to consider the possibilities of combining computer technologies with the Euler methodology and philosophy of technology. To improve the educational process, it is proposed to consider the Euler methodology as a rapidly expanding "Universe of Knowledge" using associative thinking techniques. The relationship between fundamental and applied research is clearly visible. The history of the Euler turbine demonstrates the fundamental interconnection between mathematics, technology, invention, engineering, and philosophy. Euler's multidisciplinary views on science and technology are particularly in demand today, and today there are unique digital technologies for developing Euler's complicated ideas, which were centuries ahead of their time.

Within the framework of this study, the following main tasks are set:

1 – to study the options of multiflow nozzle apparatuses designed to control the thrust vector within a full geometric sphere (including, according to the patents of the authors of this article);

2 – to consider the technical capabilities of multiple thrust tail-off (cutoff) while maintaining unchanged operating modes at the source of the working gas (or liquid).

3 – to prepare recommendations on the use of the Euler methodology in the training of modern designers.

2. Research Methodology

A flowchart describing the applied research methodology is shown in Figure 1.

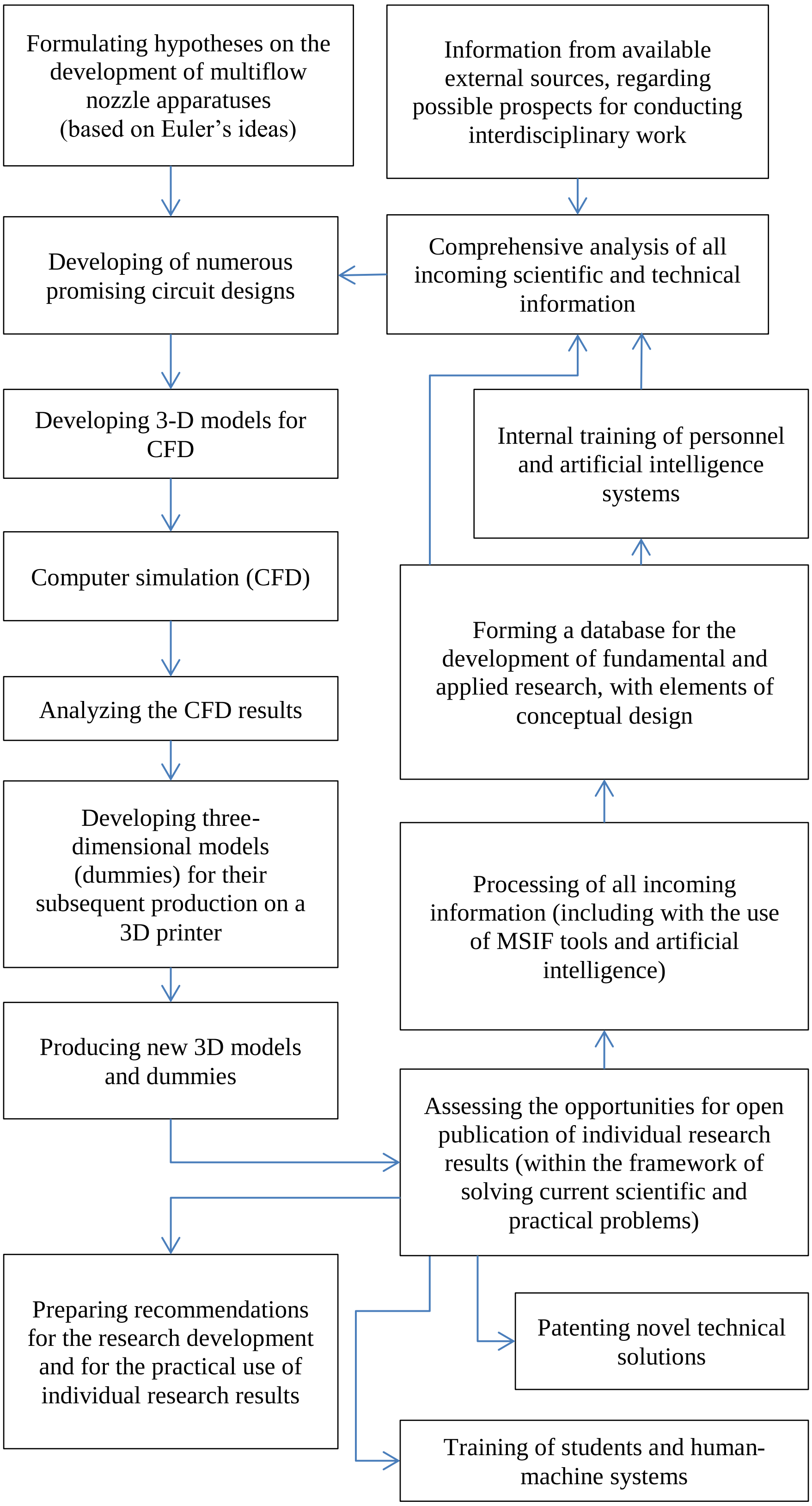

Figure 1. Flowchart of the methodology used in the research

While preparing the scientific groundwork, the authors have already shown that when using a multiflow ejector, it is possible to radically expand the range of thrust vector control, both in modulus and direction, with various options for controlling the coordinates of the initial point of the thrust vector [4-7]. At this stage of the research, an option for dividing the energy directly in the multiflow nozzle apparatus of the ejector in the zone with a higher energy density is proposed. In accordance with the flowchart (Figure 1), at the beginning of the research, a hypothesis was formulated regarding the possibility of creating a universal and simple control system for a multiflow nozzle (and a multiflow ejector, respectively) that is suitable for creating ergonomic and computerized jet systems to effectively solve various practical problems.

It is advisable to develop an Euler methodology that has been proven for centuries to withstand the onslaught of avalanche-like overproduction of information, considering the existing limits of perceiving such volumes of information (according to the physical capabilities of a human being). Together, CFD technologies, MSIF tools for digital systems [16], and artificial intelligence technologies open up new opportunities for the development of ejector systems in various industries, including power engineering [57] and aviation [3]. Three-dimensional CFD models were developed according to the flowchart (Figure 1). Subsequently, a computer simulation (CFD) was performed. The results were analyzed. Three-dimensional models (dummies) were developed for subsequent production using a 3D printer. New three-dimensional models and models are produced to test individual ideas and technical solutions, which are subsequently planned to be patented. Opportunities for open publication of individual research results are assessed (within the framework of solving current scientific and practical problems in power engineering and the development of unmanned vehicles). All incoming information is processed using MSIF tools with the prospect of adding artificial intelligence tools.

Within the framework of scientific research, in accordance with the presented methodology, the study was conducted considering a known order or sequence. A hypothesis was formed regarding the possibility of creating a basic (simplest) jet element suitable for creating reversible flow and complex high-tech jet control systems. The hypothesis is graphically formalized during the development of a circuit diagram or group (set) of circuit diagrams. The circuit diagram is then supplemented by a description of the operating principle. During the description of the operating principle, the parameters suitable for the quantitative assessment of the technological process itself were identified. The parameters can and should be grouped based on technology philosophy. Within the framework of CFD technologies, the following groups of parameters are of utmost importance: geometric parameters of channels and solid walls, and parameters characterizing the properties of fluids and the operating process as a whole. For a more in-depth analysis, the strength properties of structural materials are considered in the development of research and design, and an economic assessment is given at each stage of the product life cycle, from design to disposal. Within the framework of this study, it is not planned to raise strength analysis and economic issues. This article discusses the most important issues in jet technology related to the formation of a new direction of research on multiflow nozzle apparatuses designed to control the thrust vector within a full geometric sphere when the angle of deviation of the thrust vector can vary in the range from +180 ° to –180 °in any direction.

Further, according to the flowchart (Figure 1), with the emergence of new knowledge, databases are formed for the development of fundamental and applied research with elements of conceptual design. New information is used to train designers and to patent individual technical solutions. The research results were used for research and development in jet technology to create energy-efficient technologies for oil and gas production. Individual research has focused on the development of promising unmanned vehicles.

3. Results

3.1. Development of a Key Diagram of a Multiflow Nozzle Device

When studying a multiflow ejector [4-7], new possibilities for controlling the thrust vector within a full geometric sphere were first revealed, and new technical solutions were patented. It was shown that in a particular case; by dividing one gas (or liquid) flow into several flows, it is possible to change the direction of the thrust vector of an aircraft (or underwater vehicle). Generally, energy flows are controlled during the movement of fluids (gases or liquids) in complex gas-dynamic and hydrodynamic systems. The research results are intended for use in the oil and gas industry to improve the efficiency of technologies for hydrocarbon extraction and processing. The individual research results can be used to develop jet control systems for unmanned vehicles for various purposes. As part of the development of their own studies [4-7], the authors proposed considering a basic jet element that ensures the division of one flow (with a mass flow rate of gas at the inlet Q_0) into two flows, with mass flows $Q_a\ and\ Q_b$, respectively, as shown in Figure 2. According to Euler's methodology, the number of output channels can be designated as a variable $z = var$.

At a constant pressure, the conditions for a uniform or non-uniform gas distribution along the two outlet channels were considered.

$$\begin{cases} Q_0 = Q_a + Q_b = idem \\ \quad 0 \le Q_a \le Q_0 \\ \quad 0 \le Q_b \le Q_0 \end{cases} \tag{4}$$

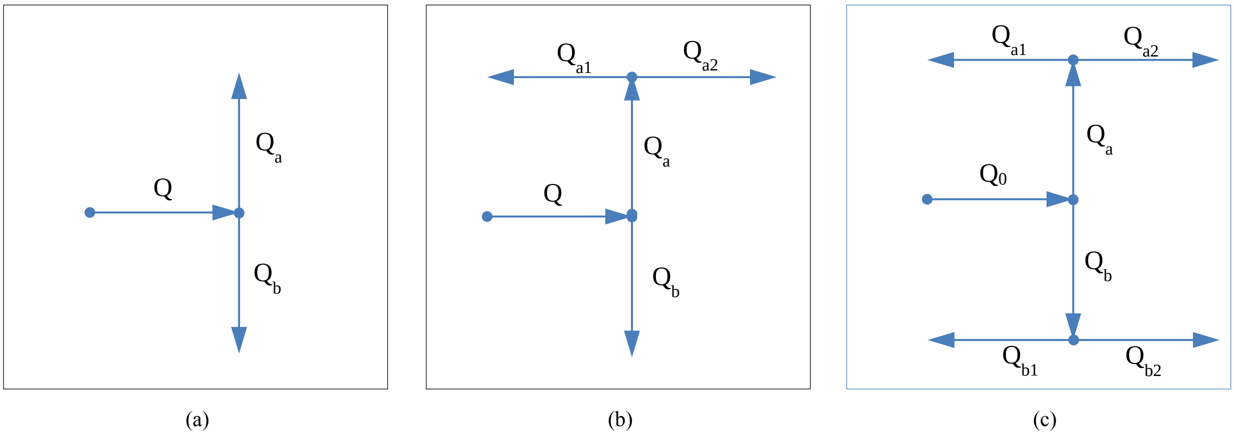

Figure 2. Schematic diagram of a multiflow nozzle apparatus: a) option with two outlet channels ($z = 2$); b) option with three outlet channels ($z = 3$); c) option with four outlet channels ($z = 4$)

When using fractal theory, it should be noted that more complex schemes are created by repeating the same basic scheme with two outlets. At constant pressure, the conditions for uniform or non-uniform gas distribution across the three outlet channels were considered ($z = 3$):

$$\begin{cases} Q_0 = Q_{a1} + Q_{a2} + Q_b = idem \\ 0 \le Q_{a1} \le Q_0 \\ 0 \le Q_{a2} \le Q_0 \\ 0 \le Q_b \le Q_0 \end{cases} \tag{5}$$

At constant pressure, the conditions for uniform or non-uniform gas distribution through the four outlet channels were considered ($z = 4$):

$$\begin{cases} Q_0 = Q_{a1} + Q_{a2} + Q_{b1} + Q_{b2} = idem \\ 0 \le Q_{a1} \le Q_0 \\ 0 \le Q_{a2} \le Q_0 \\ 0 \le Q_{b1} \le Q_0 \\ 0 \le Q_{b2} \le Q_0 \end{cases} \tag{6}$$

The technical task is to ensure controlled redistribution of flow energy among individual working chambers of a multiflow ejector owing to the flexible regulation of the hydraulic connection between the nozzle inlet channel and the working chambers, and as a consequence, to ensure regulation of the "motion quantity" parameters of flows in the cross-section at the nozzle outlet and individual working chambers, including complete shutdown of the nozzle and one or more working chambers, which are essential in emergency situations. Figure 3 shows a diagram of the jet unit (ejector). Figure 4 shows the wedge-shaped diaphragm (7a) with a square rod (8a). Figure 5 shows the outlet channel section (6a), Figure 6 shows a diagram of the jet unit after shifting the working chambers (1-3) to the left relative to nozzle 4.

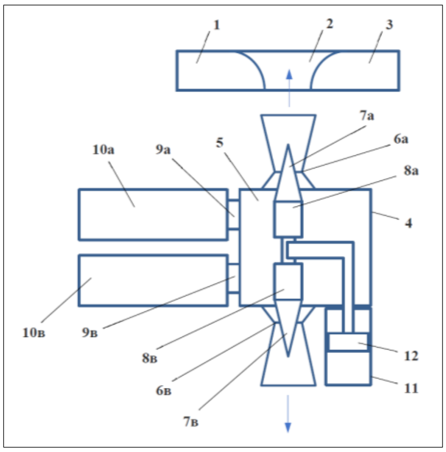

Figure 3. Schematic diagram of a jet unit: 1-3 working chambers; 4-nozzle; 5-inlet channel; 6a, 6b – outlet channels ($z = 2$); 7a, 7b – diaphragms; 8a, 8b – rod; 9a, 9b – shut-off and control devices; 10a, 10b – working fluid sources; 11 – hydraulic cylinder; 12 – piston.

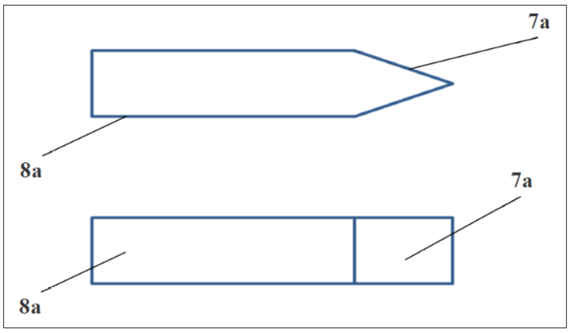

Figure 4. A version of the wedge-shaped diaphragm (7a) with a square rod (8a), according to the authors' patent (RU Patent for Invention No. 2819487)

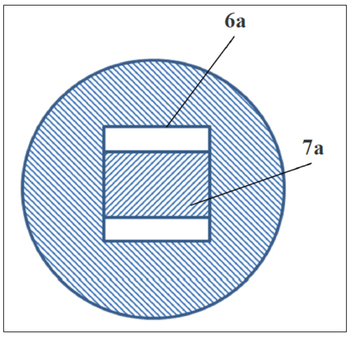

Figure 5. Cross-section of the outlet channel (6a) and diaphragm (7a), according to the authors' patent (RU Patent for Invention No. 2819487)

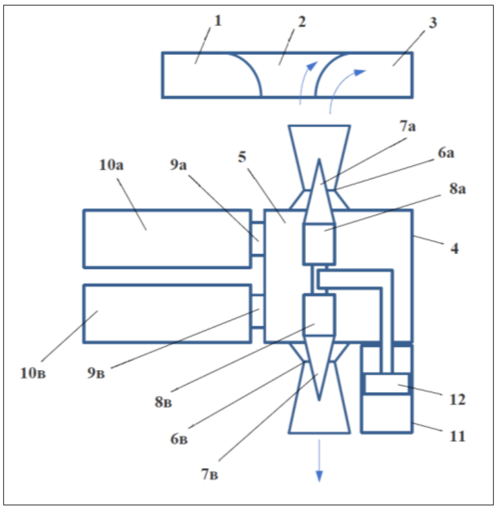

Figure 6. Schematic diagram of a jet unit: 1-3 working chambers; 4-nozzle; 5-inlet channel; 6a, 6b – outlet channels ($z = 2$); 7a, 7b – diaphragms; 8a, 8b – rod; 9a, 9b – shut-off and control devices; 10a, 10b – sources of the working fluid; 11 – hydraulic cylinder; 12 – piston.

The proposed jet unit comprises at least two working chambers (Figures 3 to 6 show three working chambers 1-3), nozzle 4 with inlet channel 5, and two (or more) outlet channels (6a, 6b) located in the cavity of nozzle 4 between inlet 5 and outlet channels (6a, 6b) of nozzle 4, two (or more) diaphragms (7a, 7b) mounted on rods (8a, 8b) equipped with a drive, with the possibility of reciprocating or angular movement of each diaphragm (7a, 7b) relative to the outlet channel (6a, 6b) of nozzle 4. Each pair of a diaphragm and a rod (pair 7a, 8a; or pair 7b, 8b) has a cross section in the form of a circle or polygon, and the outlet channel (6a or 6b) of nozzle 4, respectively, has a circular or polygonal cross section with ensured displacement of the diaphragm and the rod through the nozzle outlet channel, the complete blocking of one or more outlet channels (6a, 6b) of nozzle 4, and the adjustable direction of the working fluid flow into one of the working chambers (1-3) or simultaneously into several working chambers 1-3). In this case, inlet channel 5 of nozzle 4 is hydraulically connected through shut-off and control devices (9a, 9b) to the working fluid sources (10a, 10b), with the possibility of simultaneously supplying the working fluid from several sources (10a, 10b) to inlet channel 5 of nozzle 4, or with the possibility of sequentially connecting working fluid sources (10a, 10b) to inlet channel 5 of nozzle 4. The example in Figure 3 shows a hydraulic drive that includes hydraulic cylinders 11 and piston 12; when piston 12, where the diaphragms (7a, 7b) are also displaced relative to the outlet channel (6a, 6b) of nozzle 4, which ensures regulation of the critical section area.

The outlet channel (6a, 6b) of nozzle 4 is hydraulically connected to working chamber 1 or working chambers 2 and 3. The number of working chambers and outlet channels of the nozzle was increased.

Diaphragm 7 can be placed between inlet 5 and outlet (6a, 6b) channels of nozzle 4 with the possibility of linear and angular displacements relative to the outlet channel (6a, 6b) of nozzle 4 for a controlled change in the flow direction in the outlet channel 6 of nozzle 4 (Figure 3).

The diaphragm (7a, 7b), rod (8a, 8b), and outlet channel (6a, 6b) of nozzle 4 have different designs and shapes. For example, the diaphragm (7a, 7b) and rod (8a, 8b) have a circular or polygonal cross section, and the outlet channel (6a, 6b) of nozzle 4 has a circular or polygonal cross section, respectively, with the provided displacement of the diaphragm (7a, 7b) and rod (8a, 8b) through the outlet channel (6a, 6b) of nozzle 4, with the possibility of completely blocking the outlet channel (6a, 6b) of nozzle 4, and with the provided adjustable direction of the working fluid flow into one of the working chambers (1-3) or simultaneously into several working chambers (1-3). Working chambers (1-3) can be displaced relative to nozzle 4, as is known from prior work (for example, by analogy with the selected prototype).

In the examples in Figures 4 and 5, the diaphragm (7a, 7b), rod (8a, 8b), and outlet channel (6a, 6b) of nozzle 4 have square cross sections. It is also possible to use other geometric shapes to make diaphragm (7a, 7b), rod (8a, 8b) and outlet channel (6a, 6b), including various options with circles and polygons (square, rectangle, rhombus, pentagon or other shapes, including options with variable geometry – the so-called "morphing"). Thus, for example, the critical section (6a) can be square, and further downstream, the cross-sectional area of the outlet channel can increase (similar to a Laval nozzle), whereas the shape of the channel cross-section can change to a circle, rectangle, or another shape (which can be achieved through the use of three-dimensional printing when forming solid walls of a channel with a complex shape).

It is also possible to rotate the diaphragm (7a, 7b) and rod (8a, 8b) at constant or variable angular velocities. For the linear and angular displacements of the diaphragm (7a, 7b) and rod (8a, 8b), various known drive systems can be used; for example, a hydraulic drive, which is schematically shown in the Figures.

3.2. Explanations of the Operating Principle of the Jet Unit (Multiflow Ejector)

The jet unit operates as follows (Figures 3 to 6). The working fluid (liquid, gas, or gas-liquid mixture) was fed from the working fluid source (10a, 10b) to nozzle 4 through shut-off and control devices (9a, 9b) and inlet channel 5. The working fluid flow passed through the outlet channel (6a, 6b) of nozzle 4. From nozzle 4, the working-fluid flow was directed into the working chamber (1-3) (Figure 3). The flow directions are indicated by the arrows in the figures. In working chambers (1-3), the working fluid can be mixed with the pumped fluid, and an ejection working process is implemented in which part of the energy from the working fluid flow is transferred to the pumped fluid flow. After passing through the working chambers (1-3), the mixture of the working and pumped fluids is directed further into the process system, which is not shown in the figures.

The diaphragm (7a, 7b) can be placed between inlet 5 and outlet (6a, 6b) channels of nozzle 4 with the possibility of linear (and angular) displacement relative to the outlet channel (6a, 6b) of nozzle 4 for a controlled change in the direction of the flow in the outlet channel (6a, 6b) of nozzle 4. Working chambers (1-3) can be displaced relative to nozzle 4, as is known from prior art (for example, by analogy with the selected prototype), whereas the working fluid flow can be directed into working chambers 1, 2, or 3 depending on the technological problem being solved. The distribution of the working fluid over working chambers 1, 2, and 3 can be uniform or non-uniform, depending on the technological problem being solved.

When using the drive (11, 12), diaphragm (7a, 7b), and rod (8a, 8b), it is possible to completely block the outlet channel (6a, 6b) in the narrowest section (critical section) (Figures 2-4). In cases where the diaphragm (7a, 7b) goes beyond the critical section of the outlet channels (6a, 6b), the rod (8a, 8b) can completely block the outlet channel (6a, 6b) because the shape and dimensions of the cross-section of the rod (8a, 8b) can coincide with those of the outlet channel (6a, 6b).

Working chambers 1, 2, and 3 can be made in the form of multidirectional channels grouped in a single block, with the possibility of shifting the multidirectional channels relative to the outlet channel (6a, 6b) of nozzle 4 (Figure 5). In such cases, there are opportunities to control the thrust vector within a full geometric sphere [4-7]. Various known drive systems, such as electromagnetic or hydraulic drives (not shown in the figures), can be used for linear and angular displacements of the block from working chambers 1, 2, and 3. This provides the ability to control the change in the cross-sectional area of each outlet channel (6a, 6b) of Nozzle 4. It is also possible to maintain a constant value for the total cross-sectional area of the outlet channels (6a, 6b) with any displacement of the diaphragm (7a, 7b). Under such conditions, in a number of cases, it is possible to maintain a constant pressure inside nozzle 4 and inside the included working fluid sources (10a, 10b) while maintaining the ability to control the thrust vector by the modulus (from zero to maximum) and direction (within the full geometric sphere).

In this way, the parameters of the “motion quantity” of the flows in the cross-section at the outlet of the nozzle and individual working chambers are regulated, which is determined as the product of the mass flow rate and the flow velocity. In some cases, the diaphragm (7a, 7b) can rotate around the center of the outlet channel (6a, 6b). In this case, a pulsed (nonstationary) flow mode through working chambers 1, 2, and 3 can be implemented. Stationary flow mode was maintained in nozzle channel 4. Inlet channel 5 of nozzle 4 is hydraulically connected to the working fluid sources (10a, 10b) through shut-off and control devices (9a, 9b), with the possibility of simultaneously feeding the working fluid from several working fluid sources (10a, 10b) into inlet channel 5 of nozzle 4. In this case, the shut-off and control devices (9a) and (9b) were simultaneously open.

Provision was made for the serial connection of the working fluid sources (10a, 10b) to inlet channel 5 of nozzle 4. For example, in this case, the shut-off and control device (9a) was opened first. After the operation of the working fluid source (10a) for a specified period, the shut-off and control device (9a) is closed, and the shut-off and control device (9b) is opened. Furthermore, the next working fluid source (10b) supplied the working fluid to inlet channel 5 of nozzle 4. Depending on the technical or technological task being solved, there may be more than two working-fluid sources. For example, when developing hydrocarbon deposits, a gas (or oil) well may be considered a separate working fluid source. For example, when developing various transport systems, a gas generator (an air-breathing engine or rocket engine of a certain type) can be considered as a separate source of working fluid. In particular, in specific cases of implementing the invention, rod (8a, 8b) can be equipped with a hydraulic, mechanical, electromagnetic, electric drive, or a combined drive using combinations of the above-mentioned drive options.

Thus, the proposed multiflow nozzle apparatus solves the problem of expanding the variability of the working parameters of the flow at the nozzle outlet and at the outlet of the working chambers by providing a controlled redistribution of the flow energy among individual working chambers through the flexible regulation of the hydraulic connection between the nozzle inlet channel and working chambers.

Figure 7 shows the design scheme of the nozzle apparatus (option). The expanding part of the Laval nozzle is not shown here. The options for diaphragm positioning are as follows: a) $x_a < 0$; b) $x_a = 0$; c) $x_a > 0$; and d) $x_a > L_{1a}$.

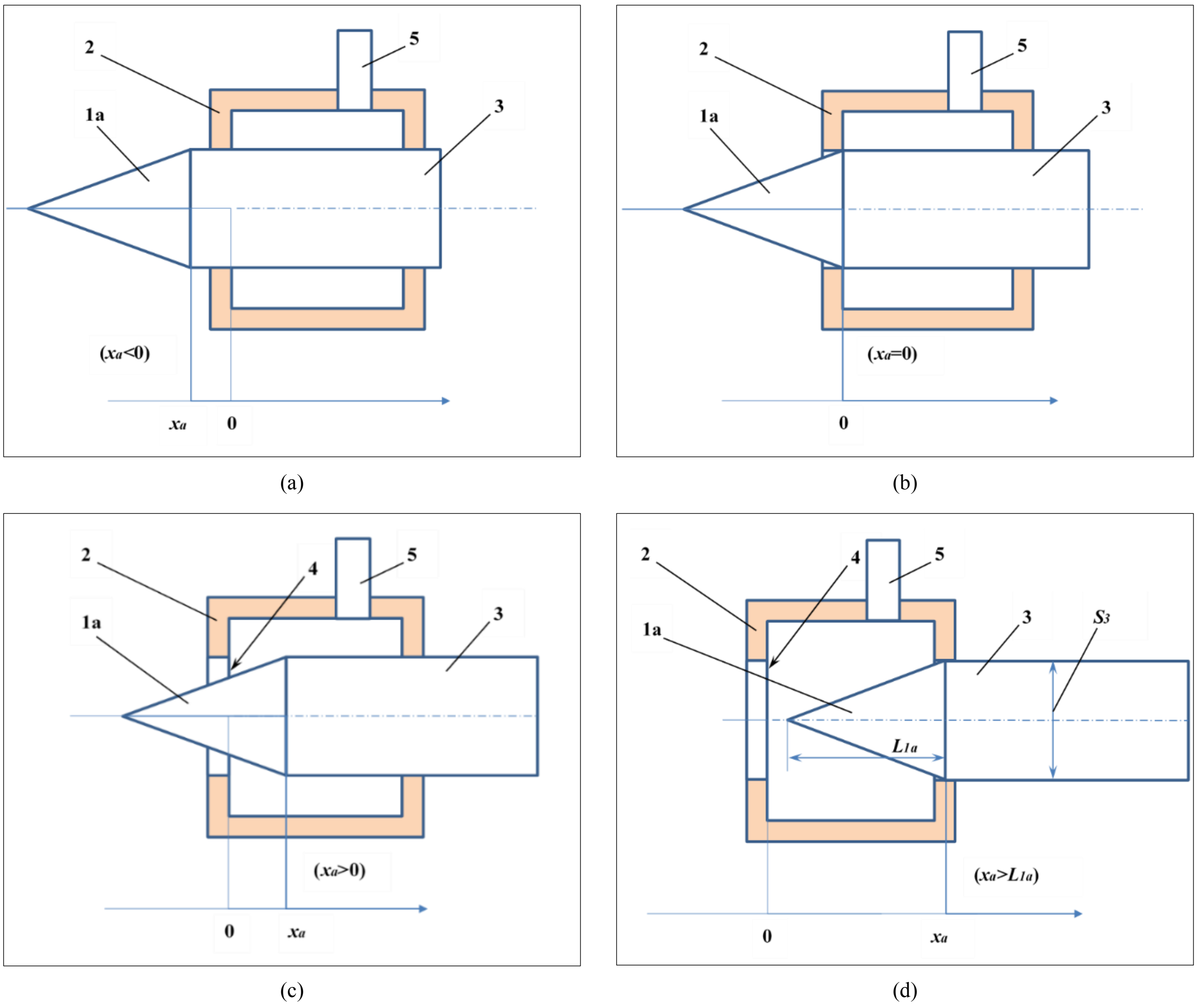

Figure 7. Nozzle apparatus diagram: 1a – diaphragm; 2 – nozzle; 3 – rod; 4 – outlet channel (critical section); 5 – inlet channel. Diaphragm positioning options: a) $x_a < 0$; b) $x_a = 0$; c) $x_a > 0$; d) $x_a > L_{1a}$

The following designations are adopted for the first output channel:

x_a – The coordinate of the base of the wedge-shaped diaphragm.

Q_a – Mass flow rate of gas through the channel (corresponding to coordinate x_a).

Q_0 – The maximum mass flow rate of gas through the channel.

S_{1a} – Size of the wedge-shaped diaphragm in the critical section.

S_{2a} – Size of the side of the square for the first outlet channel.

$\bar{F}_a$ – Thrust vector (corresponding to coordinate x_a).

F_a – The thrust vector modulus (corresponding to coordinate x_a).

The following designations are adopted for the second output channel:

x_b – The coordinate of the base of the wedge-shaped diaphragm.

Q_b – The mass flow rate of gas through the channel (corresponding to coordinate x_b).

S_{1b} – The size of the wedge-shaped diaphragm in the critical section.

S_{2b} – Size of the side of the square for the second outlet channel.

$\bar{F}_b$ – Thrust vector (corresponding to coordinate x_b).

F_b – the thrust vector modulus (corresponding to coordinate x_b).

The following designations are adopted for the rod and diaphragm:

L_{1a} – The length of the wedge-shaped diaphragm in the first channel.

L_{1b} – Length of wedge-shaped diaphragm in second channel.

L_1 – Length of the wedge-shaped diaphragm for conditions when ($L_{1a} = L_{1b} = L_1$).

L_3 – The rod length.

S_3 – Size of the side of the square of the rod cross-section.

Relative area parameters:

f_a – The relative area of the first channel.

f_b – The relative area of the second channel.

f_{ab} – The total relative area of the first and second channels.

The wedge-shaped diaphragm should hypothetically provide a linear relationship between the mass flow rate Q_a and coordinate x_a over the interval $0 \le x_a \le L_{1a}$:

$$Q_a/Q_0 = x_a/L_{1a} \tag{7}$$

$$0 \le x_a/L_{1a} \le 1 \tag{8}$$

$$0 \le Q_a/Q_0 \le 1 \tag{9}$$

In the area where $x_a \le 0$, the following condition was satisfied: $Q_a = 0$. In the area where $x_a \ge L_{1a}$, the following condition is met: $Q_a = Q_0$, for the option with the completely open outlet channel when $S_{2a} = S_3$, where S_{2a} is the dimension of nozzle channel 4.

Figure 8 shows the idealized control characteristics of the jet unit, an option in which $S_{2a} = S_3$. Additionally, it presents an option when $S_{2a} > S_3$.

The thrust vector module, $\bar{F}_a$ is designated as F_a. The wedged shape of the diaphragm should hypothetically provide a linear relationship between the nozzle thrust F_a (in the examples, the nozzle thrust module is mainly considered) and coordinates x_a in the interval $0 \le x_a \le L_{1a}$:

$$F_a/F_0 = x_a/L_{1a} \tag{10}$$

$$0 \le x_a/L_{1a} \le 1 \tag{11}$$

$$0 \le F_a/F_0 \le 1 \tag{12}$$

In the area where $x_a \le 0$, the following condition is met: $F_a = 0$, because $Q_a = 0$. In the area where $x_a \ge L_{1a}$, the following condition is met: $F_a = F_0$, for the option with a completely open outlet channel when $S_{2a} = S_3$.

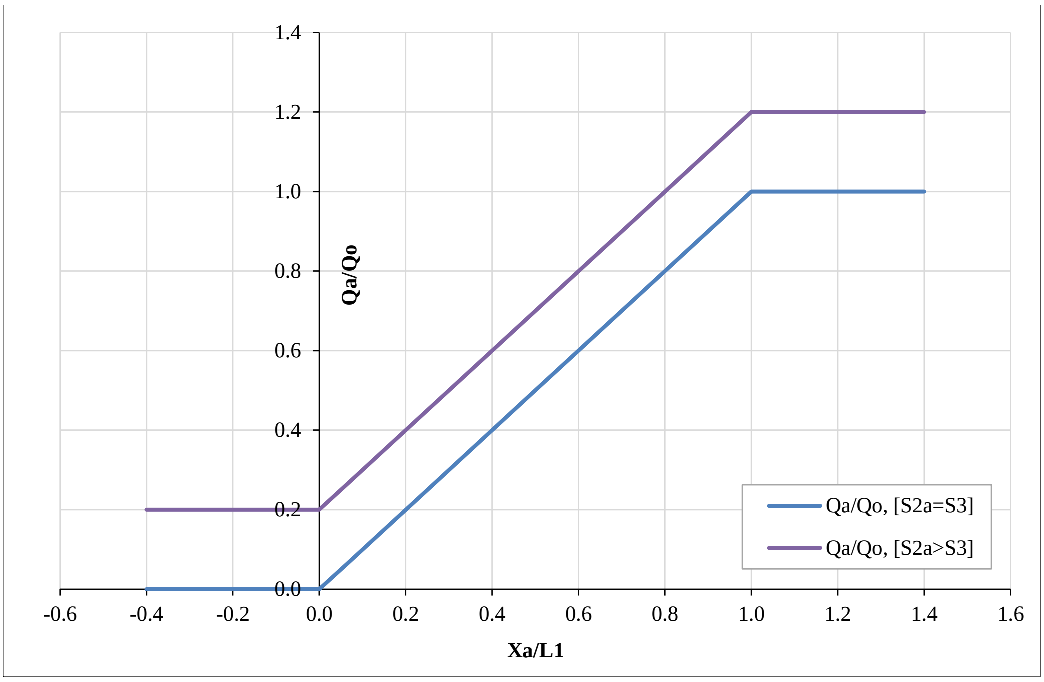

Figure 8. Control characteristics of the jet unit: option when $S_{2a} = S_3$; option when $S_{2a} > S_3$, with $L_{1a} = L_1$

Figure 9 shows the design diagram of the nozzle apparatus (an option with the possibility of flow reversal). In this example $x_b = x_a - L_{1a}$.

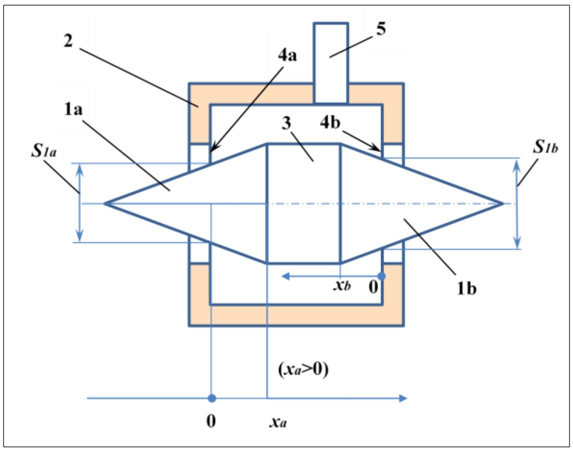

(a)

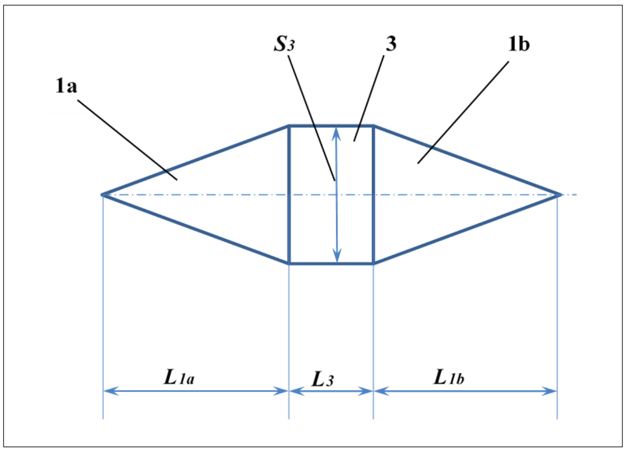

(b)

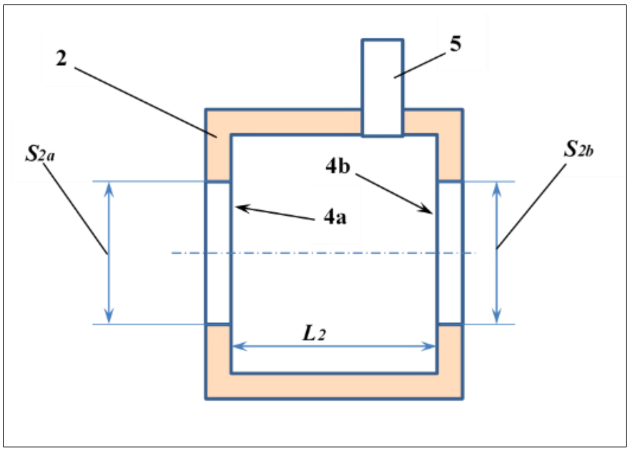

(c)

Figure 9. Schematic diagram of the nozzle apparatus (1a, 1b – diaphragms; 2 – nozzle; 3 – rod; 4a, 4b – outlet channels (critical section); 5 – inlet channel): a) design version with flow reversal; b) design version for a diaphragm system; c) design version for a housing.

The control characteristics for an idealized jet unit are presented in tabular form (Table 1) and graphically (Figures 8 to 11). The options were considered when $L_{1a} + L_3 = L_2$; and $L_{1a} = L_{1b} = L_1$.

Table 1. An example with control characteristics for an idealized jet unit

Xa/L1a	*Qa/Qo*	*Fa/Fo*	*Xb/L1b*	*Qb/Qo*	*Fb/Fo*	*Qa/Qo, [S2a>S3]*
1.40	1.00	1.00	-0.40	0.00	0.00	1.20
1.00	1.00	1.00	0.00	0.00	0.00	1.20
0.75	0.75	0.75	0.25	0.25	0.25	0.95
0.50	0.50	0.50	0.50	0.50	0.50	0.70
0.25	0.25	0.25	0.75	0.75	0.75	0.45
0.06	0.06	0.06	0.94	0.94	0.94	0.26
0.00	0.00	0.00	1.00	1.00	1.00	0.20
-0.40	0.00	0.00	1.40	1.00	1.00	0.20

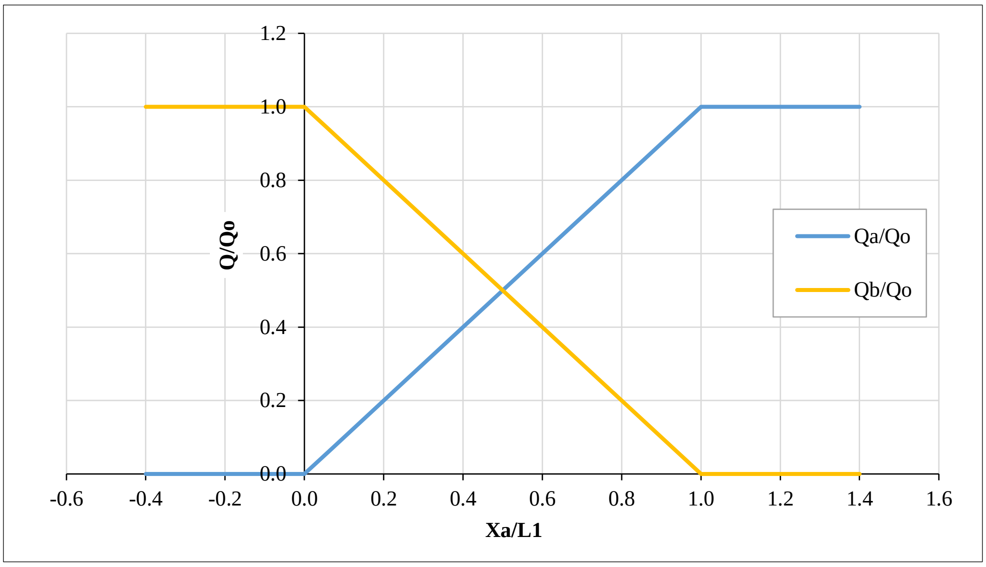

Figure 10. Control characteristics of the jet unit Q/Q_0: an option when $L_{1a} + L_3 = L_2$; with $L_{1a} = L_{1b} = L_1$

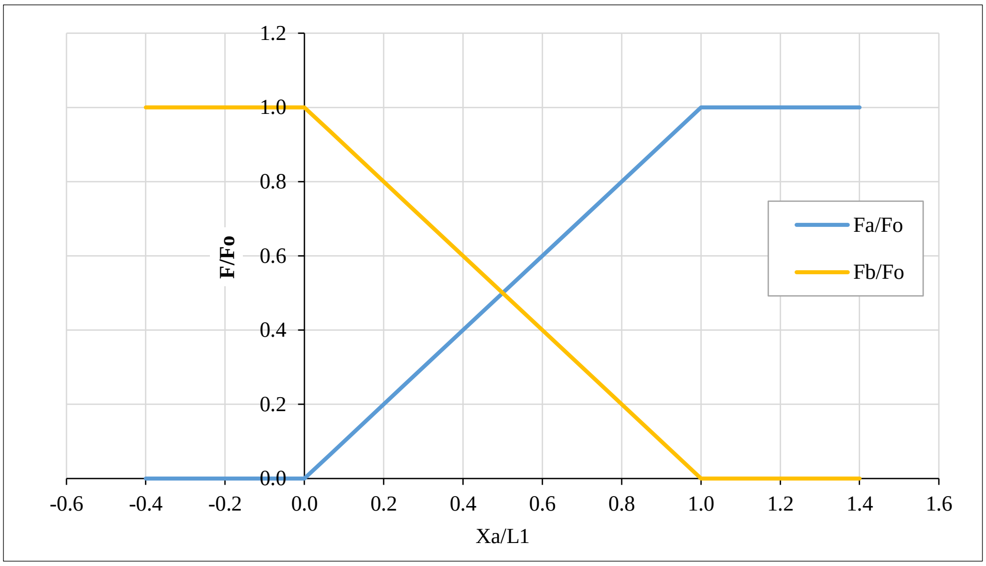

Figure 11. Control characteristics of the jet unit Q/Q_0: an option when $L_{1a} + L_3 = L_2$; with $L_{1a} = L_{1b} = L_1$

For the interval $0 \leq x_a/L_1 \leq 1$, the following relationships between the mass flow rates and thrust modules are valid:

$$Q_a + Q_b = idem \tag{13}$$

$$F_a + F_b = idem \tag{14}$$

In the examples presented, the angle between thrust vectors $\bar{F}_a; \bar{F}_b$ was 180 °for a special case. However, in the general case, the angle between the vectors $\bar{F}_a; \bar{F}_b$ can take any value, including the possibility of changing this value over time. The vector sum $\bar{F}_a + \bar{F}_b$ is determined based on the directions of these vectors in three-dimensional space and the coordinates of the initial points of these vectors. In the general case, for an aircraft, six degrees of freedom should be considered: three projections of forces on the coordinate axes in three-dimensional space and three torques relative to the coordinate axes.

In the example of a square-shaped outlet channel, the following notations and relationships for the geometric parameters can be introduced:

$$\begin{cases} x_a + L_3 + x_b = L_3 + L_{1a} = L_2 \\ x_a + x_b = L_{1a} = L_{1b} \\ \frac{x_a}{L_{1a}} = x \\ \frac{x_b}{L_{1b}} = 1 - x \\ \frac{S_{1a}}{S_{2a}} = 1 - \frac{x_a}{L_{1a}} = 1 - x \\ \frac{S_{1b}}{S_{2b}} = 1 - \frac{L_{1b} - x_a}{L_{1b}} = x \\ S_{2a} = S_{2b} \end{cases} \quad (15)$$

Cross-sectional area of the channel in housing 2:

$$\begin{cases} f_{2a} = S_{2a} * S_{2a} \\ f_{2b} = S_{2b} * S_{2b} \end{cases} \quad (16)$$

Cross-sectional area of flow channels 4a and 4b, respectively:

$$\begin{cases} f_{4a} = S_{2a} * S_{2a} - S_{1a} * S_{2a} \\ f_{4b} = S_{2b} * S_{2b} - S_{1b} * S_{2b} \end{cases} \quad (17)$$

Let us introduce the following dimensionless parameters for the relative area:

$$\begin{cases} f_a = \frac{f_{4a}}{f_{2a}} \\ f_b = \frac{f_{4b}}{f_{2b}} \\ f_{ab} = f_a + f_b \end{cases} \quad (18)$$

In this case, in the example of a square-shaped outlet channel in a coordinate system with dimensionless parameters, we can write the following functional dependencies:

$$\begin{cases} f_a = x \\ f_b = 1 - x \\ f_{ab} = 1 \end{cases} \quad (19)$$

The calculated characteristics of the nozzle apparatus with square channels for this example are presented in Figure 12.

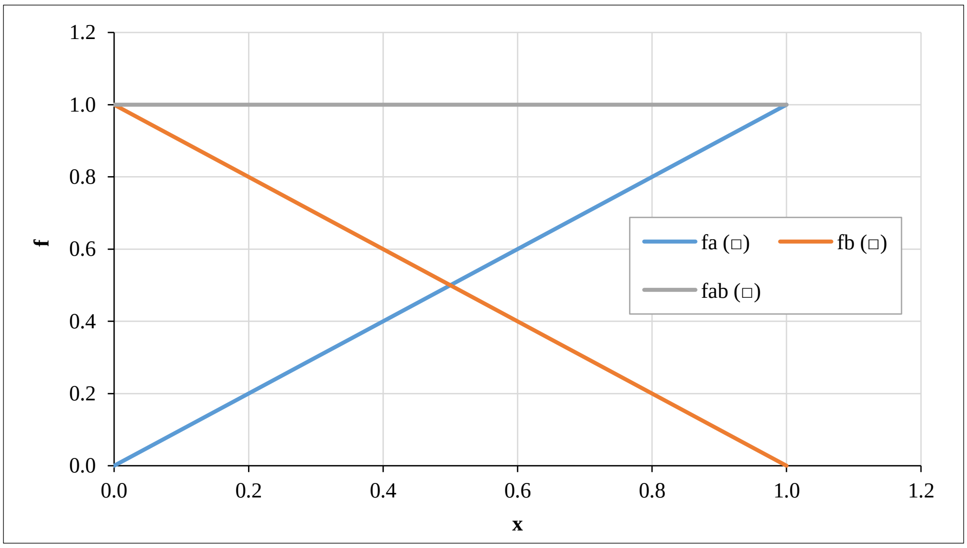

Figure 12. Control characteristics of the nozzle apparatus of type $f(x)$, with square channels (the option with a square cross-section corresponds to an additional marker □)

The presented dimensionless coordinate system is convenient for comparing nozzle apparatuses with different cross-sectional shapes of flow channels.

3.3. Computer Simulation

A solid three-dimensional model was developed for the computer simulation, as shown in Figure 13. All dimensions are in millimeters.

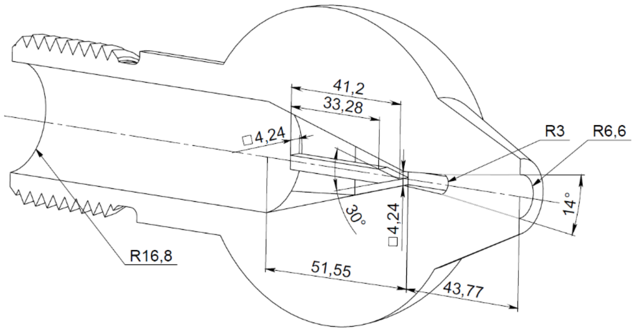

Figure 13. A controlled jet unit schematic (option)

The critical section of the nozzle had a square shape with a side of 4.24 mm. There was an expanding section behind the critical section where the square shape smoothly turned into a circle with a radius of 3 mm. Furthermore, there is a diffuser section downstream, such as the Laval nozzle, with a cone angle of 14 °. The working gas (model fluid is air) at the nozzle inlet had pressures of P=6 MPa (option 1) and P=12 MPa (option 2) at a temperature of T=2000 °C. The pressure at the nozzle outlet was 101325 Pa and the ambient temperature was 20 °C.

- Software Product (computational program): Flow Simulation 2018 SP5.0
- CPU type (processor): Intel(R) Core (TM) i5-6200U CPU at 2.30GHz
- CPU speed: 2401 MHz
- RAM (random access memory): 8065 MB
- Operating system: Windows 10

The “k-e” turbulence model was used. A computational grid was automatically built. The total number of cells was > 700,000. The computation time for one operating mode was greater than 8000 s. The number of iterations was 1000.

The results of the computer simulation are partially presented in tabular form (Tables 2 and 3) and graphically (Figures 14 to 24).

Table 2. Computer simulation results for a jet unit at a working gas pressure of 6 MPa

Xa (mm)	*Qa* (kg/s)	*Fa* (N)	*Xa/L1*	*Fa/Fo*	*Qa/Qo*
8.00	0.0886	161.138	1.000	1.000	1.000
6.00	0.0665	119.497	0.750	0.742	0.750
4.00	0.0425	74.161	0.500	0.460	0.480
2.00	0.0207	32.251	0.250	0.200	0.233
0.50	0.0051	6.817	0.063	0.042	0.058
0.00	0.0000	0.000	0.000	0.000	0.000

Table 3. Computer simulation results for a jet unit at a working gas pressure of 12 MPa

Xa (mm)	*Qa* (kg/s)	*Fa* (N)	*Xa/L1*	*Fa/Fo*	*Qa/Qo*
8.00	0.1777	338.441	1.000	1.000	1.000
6.00	0.1359	259.122	0.750	0.766	0.765
4.00	0.0854	163.146	0.500	0.482	0.480
2.00	0.0416	76.281	0.250	0.225	0.234
0.50	0.0104	15.883	0.063	0.047	0.058
0.00	0.0000	0.000	0.000	0.000	0.000

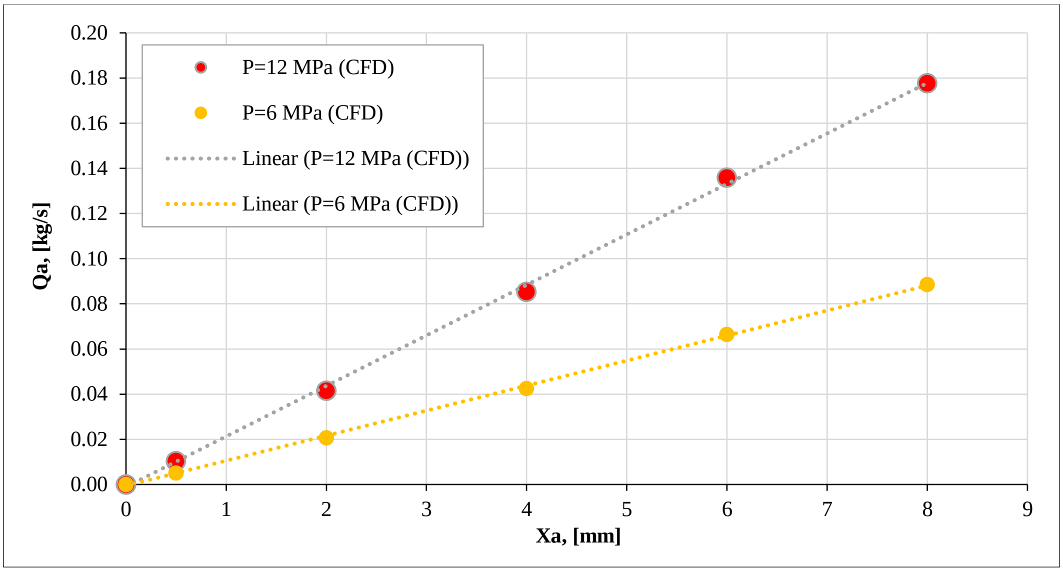

Figure 14. Control characteristics of the jet unit $Q_a(x_a)$ based on the results of CFD computer simulation

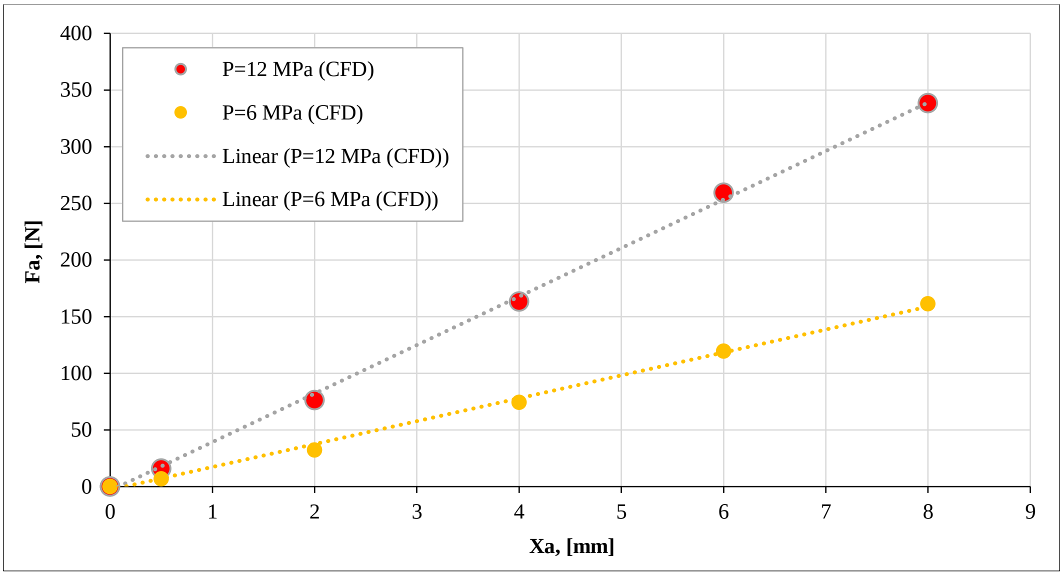

Figure 15. Control characteristics of the jet unit $F_a(x_a)$ based on the results of CFD computer simulation

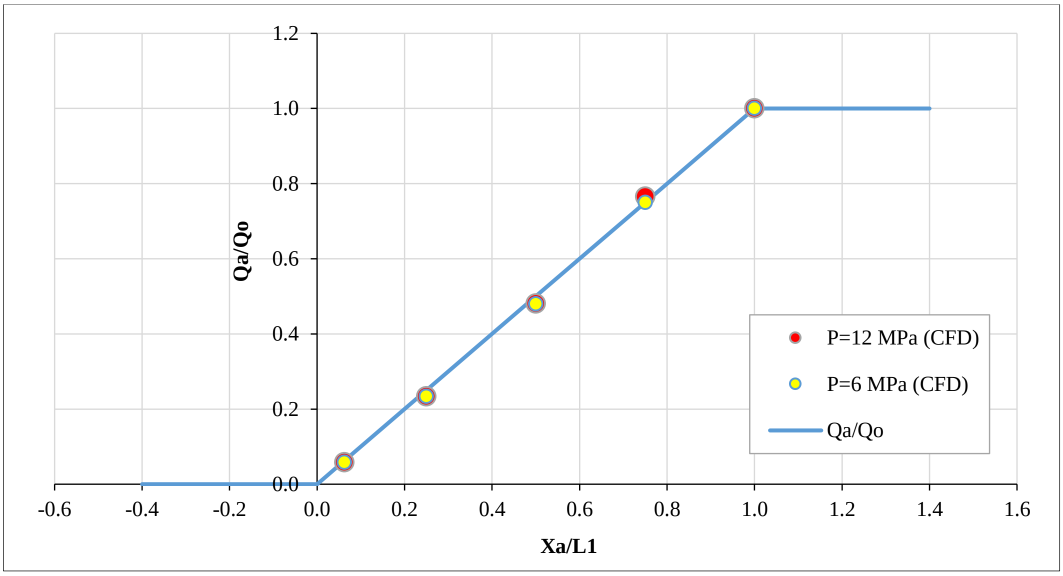

Figure 16. Control characteristics of the jet unit Q_a/Q_0 together with the CFD computer simulation results: option when $L_{1a} + L_3 = L_2$; with $L_{1a} = L_{1b} = L_1$

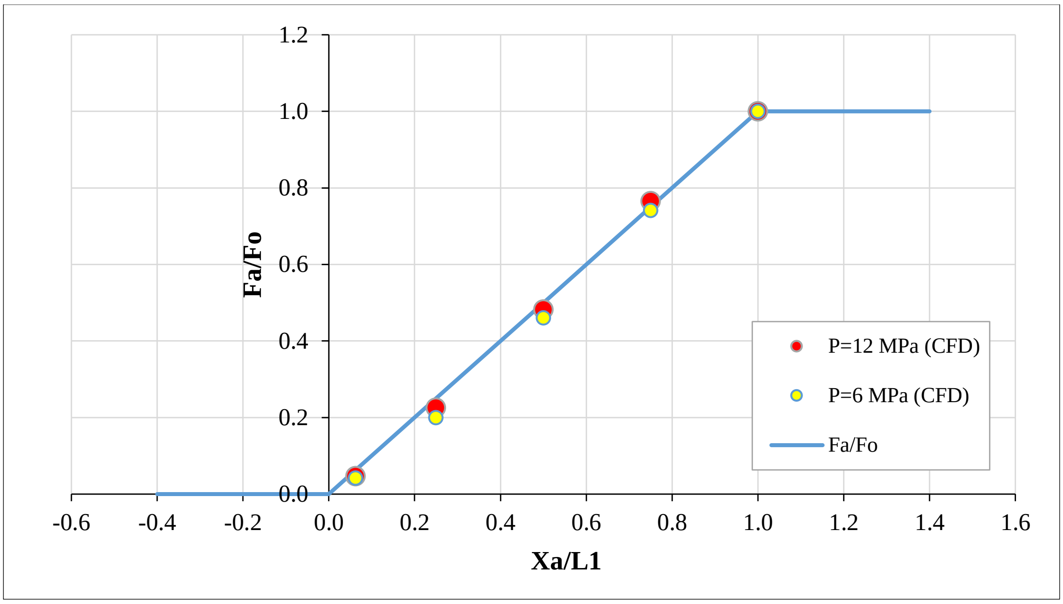

Figure 17. Control characteristics of the jet unit F_a/F_0 together with the CFD computer simulation results: option when $L_{1a} + L_3 = L_2$; with $L_{1a} = L_{1b} = L_1$

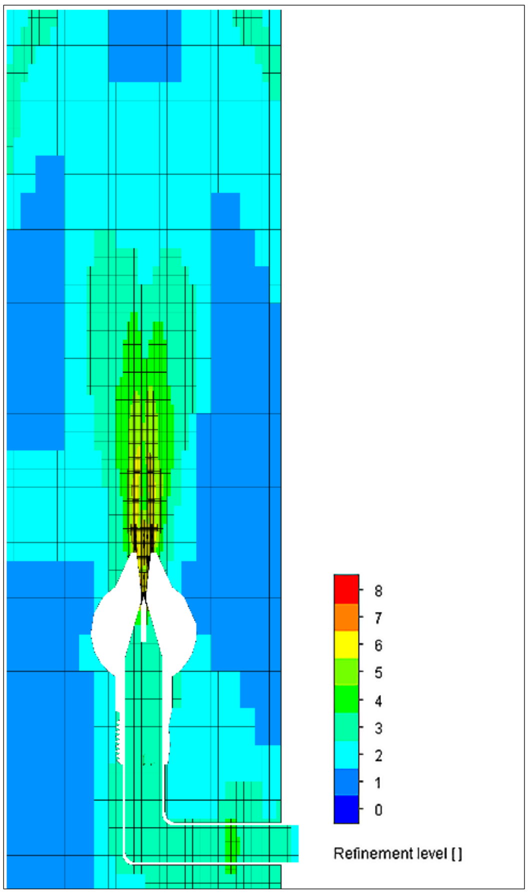

Figure 18. Computer simulation results. Computational grid, $x_a = 4$ mm, P=12 MPa

Data collection began to compare individual results obtained in the CFD computer simulation using the Flow Simulation 2018 SP5.0, and the Star CCM+ software package. At the initial stage of the research, a conclusion was made regarding the advisability of using these two software packages for patenting and the necessary verification of the operability of the new reversible nozzle (and multiflow ejector). We will assess the accuracy of computer calculations as data accumulate, understanding that increasing the accuracy of calculations is accompanied by growing financial costs for labor-intensive calculations, and considering the fact that a numerical experiment today cannot yet completely replace a physical experiment conducted on a bench setup (or in a wind tunnel).

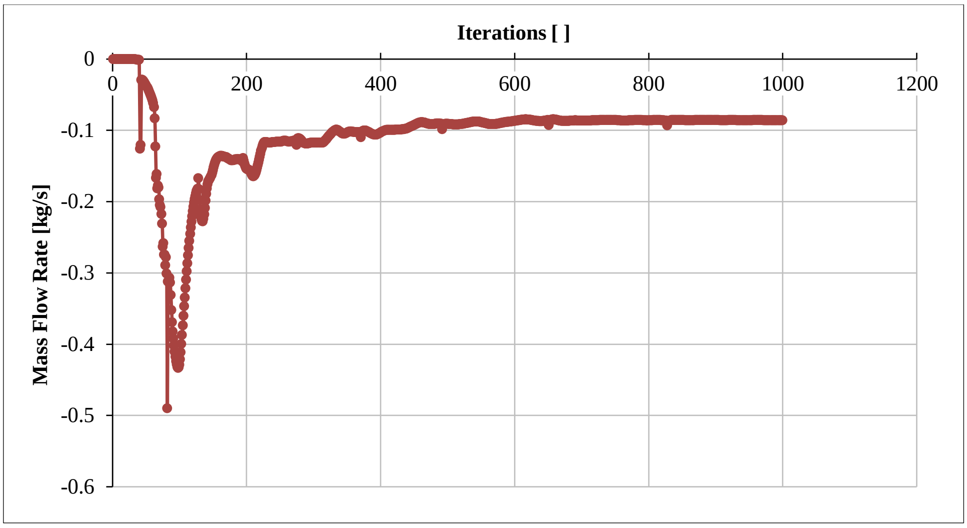

Figure 19. Computer simulation results. Mass flow convergence graph, $x_a = 4$ mm, P=12 MPa

According to the example presented in Figure 15, the obtained results make it possible to speak about the possibility of using the linear dependence $F_a(x_a)$ for pressures P=6 MPa and P=12 MPa. Similar linear dependences $F_a(x_a)$ were obtained for options P=1.5 MPa and P=3 MPa. According to the example presented in Figure 16, the obtained results make it possible to speak about the possibility of using the linear dependence Q_a/Q_0 for pressures P=6 MPa and P=12 MPa. Similar linear dependences Q_a/Q_0 were obtained for options P=1.5 MPa and P=3 MPa. In the zone $(1.0 \leq x_a/L_1 \leq 1.4)$ the outlet channel is completely open and the effect of the diaphragm on the flow can be neglected (but this assumption will be checked as the research continues). In the zone $(-0.4 \leq x_a/L_1 \leq 0)$ the outlet channel is completely closed.

According to the example presented in Figure 17, the obtained results make it possible to speak about the possibility of using the linear dependence F_a/F_0 for pressures P=6 MPa and P=12 MPa. Similar linear dependences F_a/F_0 were obtained for options P=1.5 MPa and P=3 MPa. In the zone $(1.0 \leq x_a/L_1 \leq 1.4)$ the outlet channel is completely open and the effect of the diaphragm on the flow can be neglected (but this assumption will be checked as the research continues). In the zone $(-0.4 \leq x_a/L_1 \leq 0)$ the outlet channel is completely closed. The calculation grid, as shown in Figure 18, was built automatically. The influence of the grid quality on the calculation accuracy was not assessed at this stage of the research for the reasons noted above in the text. The convergence graph shown in Figure 19 was constructed automatically, taking into account the automatically constructed computational grid shown in Figure 18.

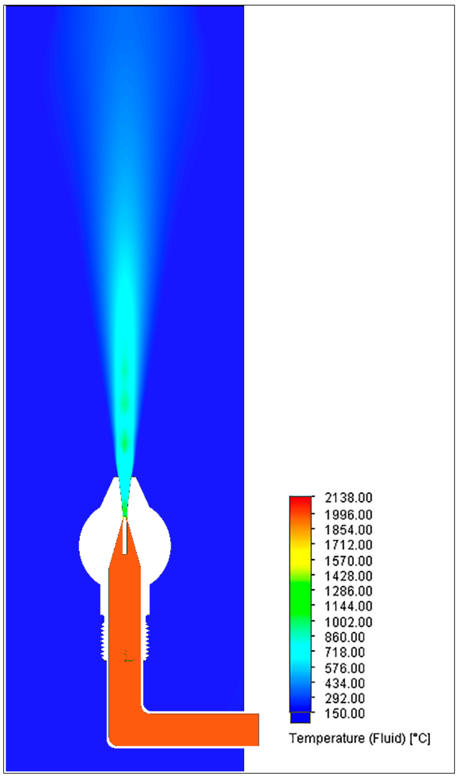

Figure 20. Computer simulation results. Temperature distribution, $x_a = 4$ mm, P=12 MPa

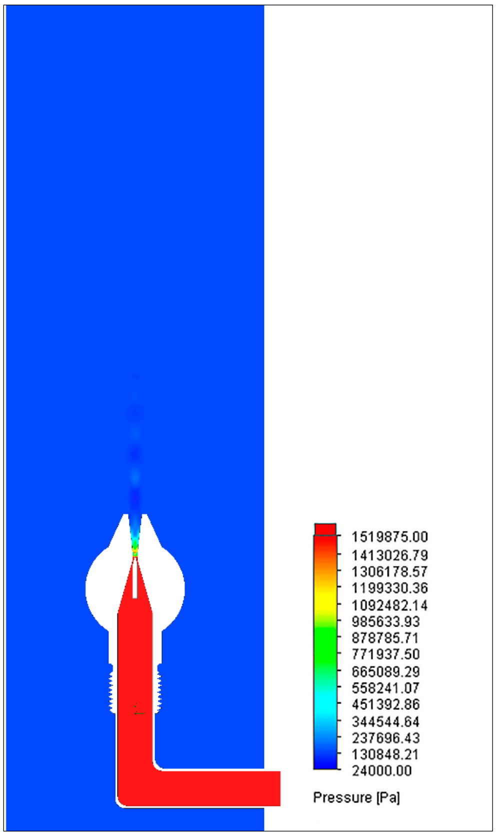

Figure 21. Computer simulation results. Pressure distribution, $x_a = 4$ mm, P=12 MPa

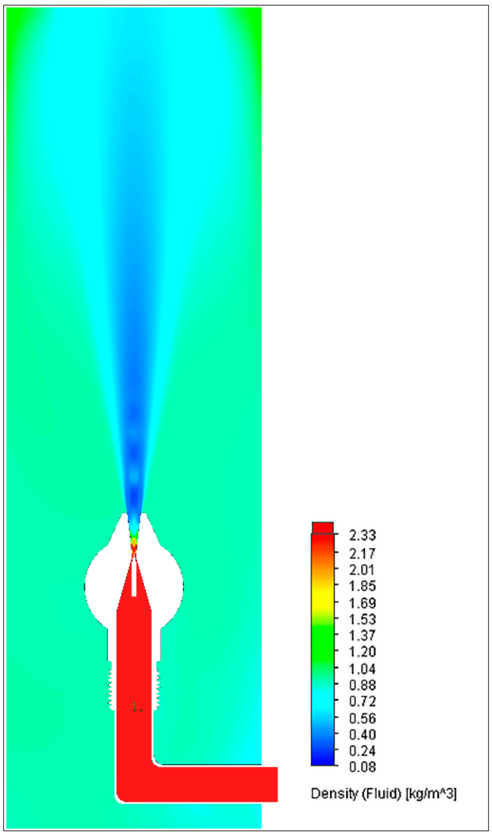

Figure 22. Computer simulation results. Computational grid, $x_a = 4$ mm, P=12 MPa

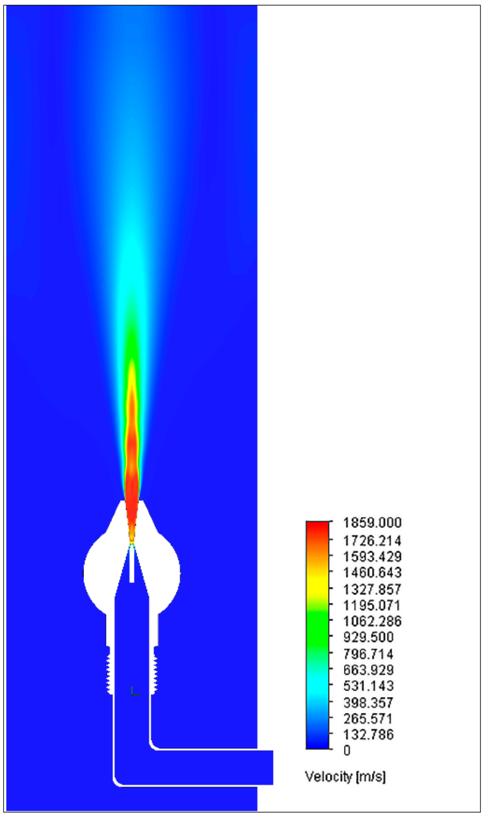

Figure 23. Computer simulation results. Velocity distribution, $x_a = 4$ mm, P=12 MPa

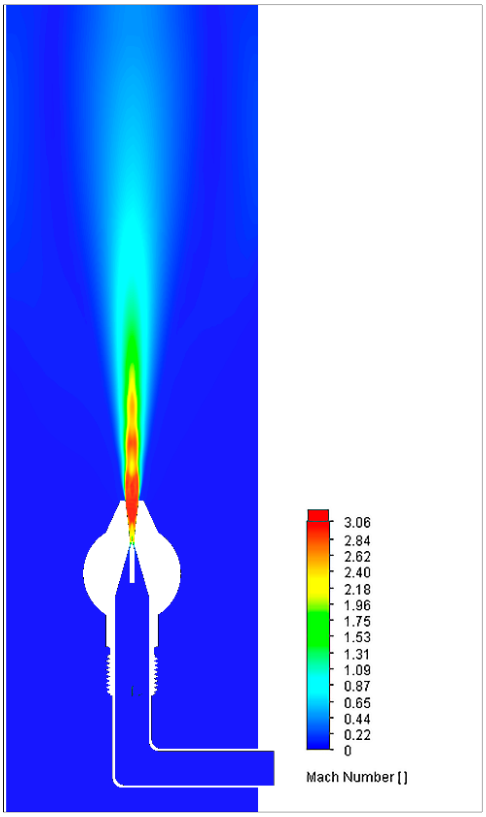

Figure 24. Computer simulation results. Mach number distribution, $x_a = 4$ mm, P=12 MPa

According to the presented example, the obtained results make it possible to discuss the possibility of using the linear dependence $Q_a(x_a)$ for pressures P=6 MPa and P=12 MPa. Similar linear dependences were obtained for options P=1.5 MPa and P=3 MPa. At this stage of the research, the main task was to check the operability of the experimental nozzle apparatus intended for use in a multiflow ejector, as this test provides the basis for patenting new technical solutions and for continuing and developing conceptual research. As is known, the requirement to improve the accuracy of calculations becomes increasingly stringent in the development of design work, in the transition from conceptual design to draft design, and then to a working project. At this stage of scientific research, data that will be used for machine learning, the educational process in the training of designers, and solving optimization problems are accumulated.

At this stage of the study, the working gas temperature at the nozzle inlet was assumed to be constant and equal to T=2000°C. While continuing the research, we plan to consider other operating modes with other values of the working gas temperature. For example, for the technology of natural gas production and preparation, the conditions of gas outflows at low temperatures, with values below zero degrees Celsius, are of practical interest. During the computer simulation (Figure 21), the gas pressure in the environment was assumed to be constant and equal to 101325 Pa. When continuing this research, other operating modes should be considered. For production technologies, conditions with an excess pressure of several MPa or several dozens of MPa are of practical interest. With regard unmanned aerial vehicles, it will be necessary to consider the natural decrease in atmospheric pressure, air density, and air temperature with an increase in flight altitude in a standard atmosphere.

During the computer simulation (Figure 22), the gas (air) density in the environment is assumed to be constant and corresponds to the parameters of a standard atmosphere at a pressure of 101325 Pa. When continuing this research, we plan to consider other operating modes with gas density in the environment at high pressures of several MPa or several dozens of MPa. During the computer simulation, the gas flow velocity at the nozzle outlet in the above examples was higher than the speed of sound, and the Mach number exceeded 1 (see Figures 23 and 24).

At the development and patenting stage of new technical solutions, the considered examples were selected to confirm the operability of these technical solutions. Such examples do not constitute any limitations in the area of practical use of the invention and scientific information. From the known level of technology, it is clear to an expert that the discussed technical solution can be implemented in practice at low values of velocities, pressures, and temperatures in the area of micromachinery inclusive; however, it can also be implemented in practice at extremely high achievable values of velocities, pressures, and temperatures in the area of powerful transportation systems inclusive (with appropriate clarifications in mathematical models, and with the appropriate selection of construction materials).

4. Discussion

4.1. Discussion of the Intermediate Results

Summarizing the intermediate results, the following can be stated: 1) the options of developed and patented jet systems designed to control the thrust vector within a full geometric sphere (according to the authors' patents, including RF Patent No. 2819487) were investigated; 2) individual technical capabilities for redistributing energy between two hemispheres were considered, with the placement of wedge-shaped control elements in the zone with high energy density in the zone of the critical section of the nozzle; 3) technical capabilities for multiple thrust tailoffs (cutoffs) were considered, while maintaining unchanged operating modes at the source of the working gas (or liquid) – options for regulating the nozzle apparatus with a constant working gas pressure and a constant total mass flow rate of the working gas were considered. At this stage of the research, tasks were set to test the hypotheses and check the operability of the patented technical solutions. We plan to solve the optimization problems during the subsequent transition from the scientific research stage to the experimental design stage.

To improve the educational process, using associative thinking techniques, it is proposed to consider the Euler methodology as a kind of the "Universe of Knowledge," which is expanding with acceleration because of CFD technologies in particular, and because of mathematics in general. Descartes [9] drew attention to the fact that, among all those who sought truth in the sciences, only mathematicians managed to find evidence. As for experiments, René Descartes noted that they (experiments) are all the more necessary, the further we advance in knowledge, and our concerns should extend beyond the present time, to do what will bring more benefit to our descendants [9]. There can be no truths so distant that they are unattainable, nor a secret that they cannot be revealed [9]. According to Euler, formulas (1-3) reinforce this statement. Within the framework of the present study, separate recommendations on the use of the Euler methodology for training modern designers were prepared, with an emphasis on the active practical application of CFD technologies, including the development of artificial intelligence and the modern philosophy of technology. The authors associated the continuation of research in the field of jet systems for thrust vector control with a comprehensive consideration of the problems of three degrees of freedom in three-dimensional space in combination with Euler angles.

In one particular case, a nozzle apparatus with two outlet channels was considered. In future research, we plan to consider options with three (or more) outlet channels to expand the capabilities of maneuvering unmanned vehicles in a three-dimensional space.

Research has begun to plan the trajectory of an aircraft when controlling the thrust vector within a full geometric sphere using the described technology for thrust cutoff (tailoff). One of the virtual training examples is presented graphically in Figure 25. The computer study was conducted in the Star CCM+ software package using DFBI – Dynamic Fluid Body Interaction on a computer with the following parameters: CPU: AMD Ryzen 9 5900X 12-Core; RAM: 64

GB; Operating system: Windows 10. The total number of cells was 6.5 million. The calculation was performed in the unsteady implicit mode using the ideal compressible gas model described by the Reynolds-averaged Navier-Stokes equations for turbulence. Air was selected as the fluid from the software package library; its dynamic viscosity, molecular weight, thermal conductivity, Prandtl number, and specific heat capacity were constants specified automatically. Pressure was 0.1 MPa and the temperature was 20°C. The K-epsilon model is used as the turbulence model (for any y+). The specified forces were applied to the center of the object under study (a sphere with a radius of 200 mm and mass of 1 kg). We plan to present a more detailed description of these numerical experiments in our future publication.

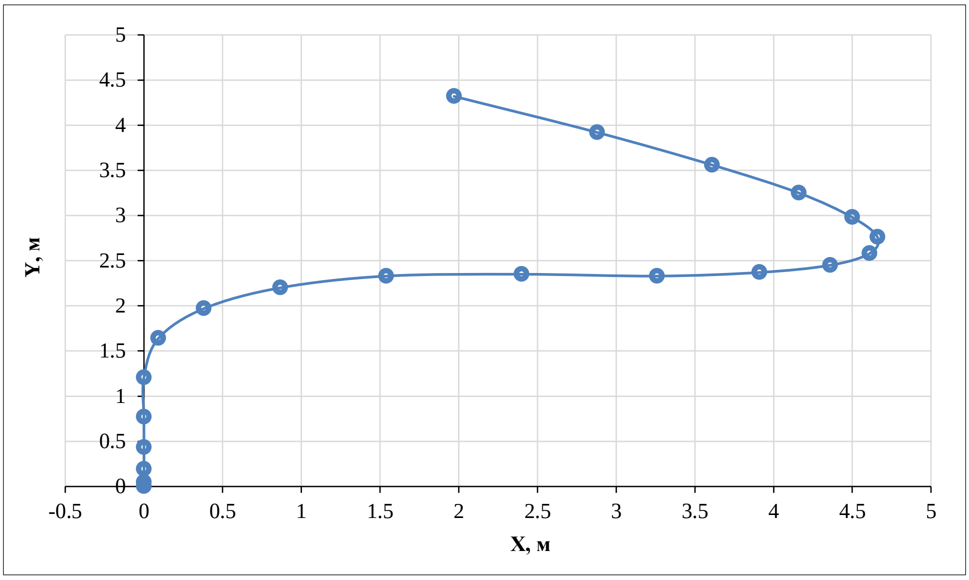

(a)

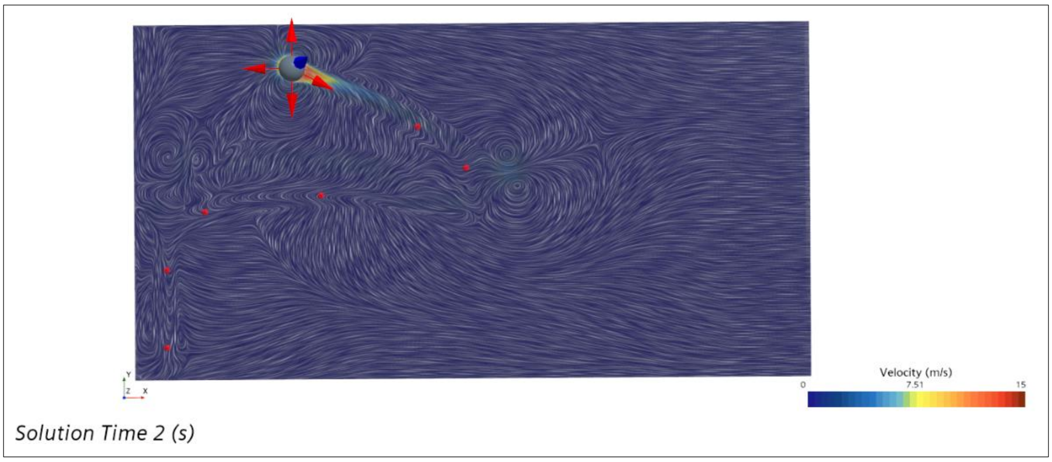

(b)

Figure 25. Computer simulation results (training sample): a) the calculated trajectory of the object movement, for two seconds; b) the velocity palette 2 seconds after the start of the object movement

The coordinates (X, Y) of the object in space are calculated at a time interval of 0.1 seconds. Coordinates (Z) in this example did not change. In Figure 25-b, the trajectory of the spherical object is highlighted using several small red markers. This training sample showed the vertical takeoff of the sphere, left-to-right movement horizontally, and right-to-left movement with a gain in altitude.

A number of numerical CFD experiments were also performed for a delta-wing UAV equipped with a thrust-vector control system, with any thrust-vector deflection angle within a full geometric sphere. The materials were prepared for publication. The individual capabilities of performing extreme maneuvers were preliminarily assessed. Thus, calculations have shown that during horizontal flight, such a UAV can rotate around a vertical axis passing through the center of the fuselage. The possibility of UAV flight and hovering in air at any angle in the direction, roll, and pitch has been theoretically shown, with the ability to perform vertical takeoff and landing in any of these positions with all possible combinations of the listed angles. It can be preliminarily (or presumably) stipulated that many maneuvers will be beyond the human capabilities of the operator, but these extreme maneuvers will be the subject (topic) of a competition between various artificial intelligences.

In most cases, a well-known version with a round nozzle cross-section is considered when creating an ejector with an adjustable nozzle cross section [57]. Figure 26 shows the calculation scheme for a multiflow nozzle apparatus made using the well-known design of a nozzle with a round cross-section.

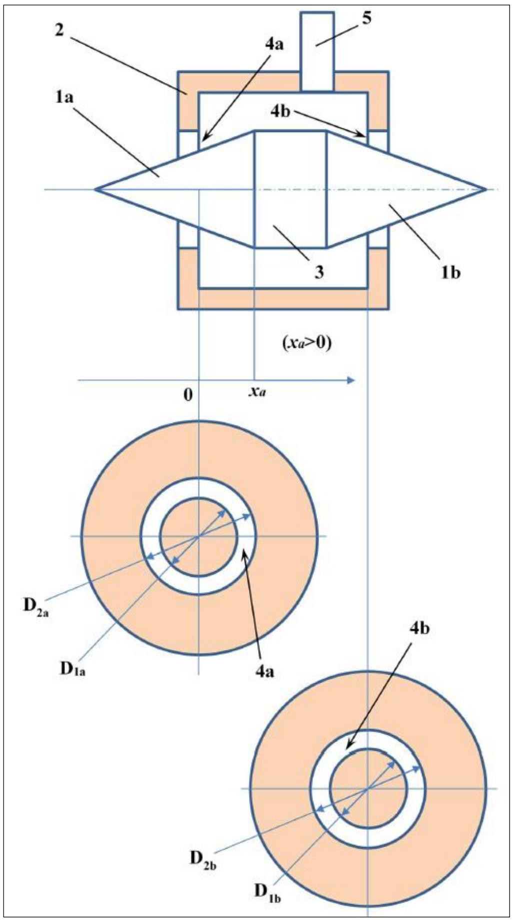

Figure 26. Schematic of nozzle apparatus with circular cross-section of channels: 1a, 1b – conical diaphragms with diameters at bases D_{1a}, D_{1b}, respectively; 2 – housing with two circular outlet channels, with diameters D_{2a}, D_{2b}, respectively; 3 – round rod, in this example with diameter D_{2a}; 4a, 4b – annular outlet channels; 5 – inlet channel.

In this example, regarding the above designations, the following conditions are highlighted:

$$\begin{cases} x_a + L_3 + x_b = L_3 + L_{1a} = L_2 \\ x_a + x_b = L_{1a} = L_{1b} \\ \frac{x_a}{L_{1a}} = x \\ \frac{x_b}{L_{1b}} = 1 - x \\ \frac{D_{1a}}{D_{2a}} = 1 - \frac{x_a}{L_{1a}} = 1 - x \\ \frac{D_{1b}}{D_{2b}} = 1 - \frac{x_b}{L_{1b}} = 1 - \frac{L_{1a} - x_a}{L_{1b}} = x \\ D_{2a} = D_{2b} \end{cases} \tag{20}$$

Cross-sectional area of the channel in the housing 2:

$$\begin{cases} f_{2a} = \pi * \frac{D_{2a}^2}{4} \\ f_{2b} = \pi * \frac{D_{2b}^2}{4} \end{cases} \tag{21}$$

Cross-sectional area of the flow channels 4a, and 4b, respectively:

$$\begin{cases} f_{4a} = \pi * \frac{D_{2a}^2 - D_{1a}^2}{4} \\ f_{4b} = \pi * \frac{D_{2b}^2 - D_{1b}^2}{4} \end{cases} \tag{22}$$

The following dimensionless parameters for the relative area are used, as in the example with a square cross-section of the channel:

$$\begin{cases} f_a = \frac{f_{4a}}{f_{2a}} \\ f_b = \frac{f_{4b}}{f_{2b}} \\ f_{ab} = f_a + f_b \end{cases} \tag{23}$$

In this case, in an example of a circular outlet channel in a coordinate system with dimensionless parameters, the functional dependencies can be written as

$$\begin{cases} f_a = 2x - x^2 \\ f_b = 1 - x^2 \\ f_{ab} = 1 + 2x - 2x^2 \end{cases} \tag{24}$$

The calculated characteristics of the circular-channeled nozzle apparatus for this example are presented graphically in Figures 27 to 29. In addition, these data were compared with the calculated characteristics of a square-channeled nozzle apparatus. The results are presented in tabular (Table 4) and graphical form. An additional marker (□) corresponds to the option with a square cross-section in the notation. An additional marker (○) corresponds to an option with a circular cross section in the notation.

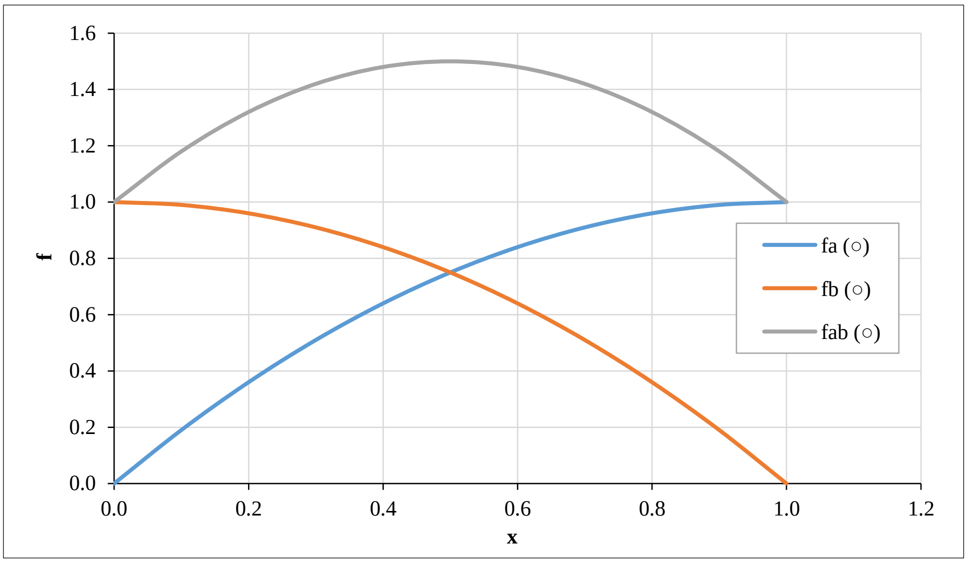

Figure 27. Control characteristics of the circular-channeled nozzle apparatus of $f(x)$ type; an additional marker (○) corresponds to the option with a circular cross-section

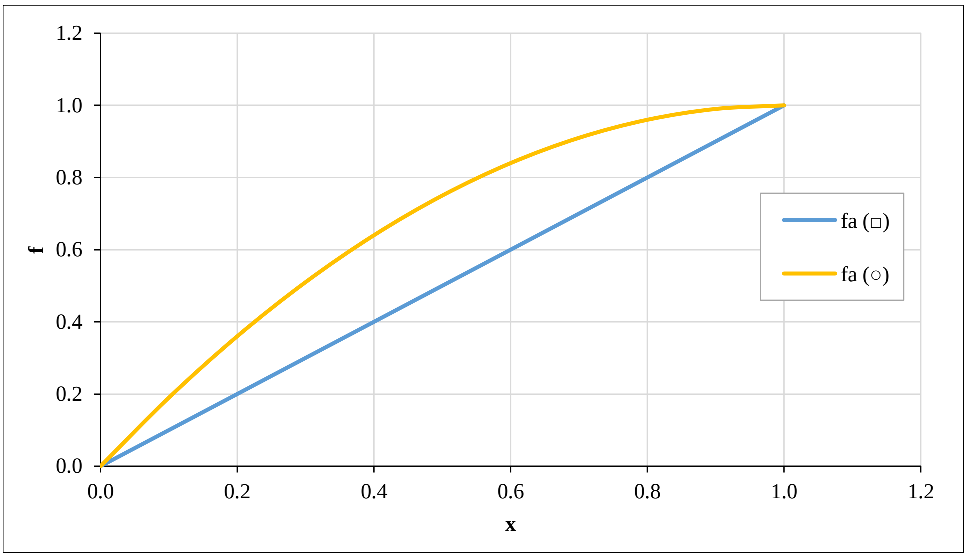

Figure 28. Control characteristics of the nozzle apparatus for one channel of $f_a(x)$ type: an additional marker (○) corresponds to the option with a circular cross-section; an additional marker (□) corresponds to the option with a square cross-section.

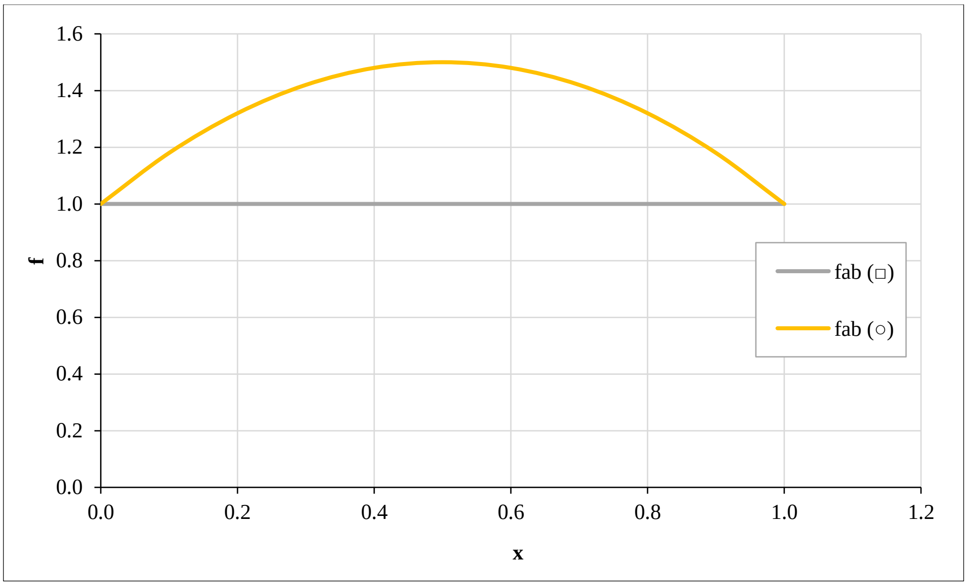

Figure 29. Control characteristics of the nozzle apparatus for two channels of $f_{ab}(x)$ type: an additional marker (○) corresponds to the option with a circular cross-section; an additional marker (□) corresponds to the option with a square cross-section.

The chosen dimensionless coordinate system was found to be convenient for comparing nozzle apparatuses with different cross-sectional shapes of flow channels.

The calculations showed that the known version with a round nozzle cross-section [57], when adjusting the position of the conical diaphragm, does not ensure the constancy of the total area $f_{ab}(x)$. Such a multiflow nozzle apparatus, with a constant gas (liquid) pressure at the inlet, does not ensure the fulfillment of the conditions $Q_0 = Q_a + Q_b = idem$; however, $Q_a = var$. The inconsistency of the parameters $(1 \leq f_{ab}(x) \leq 1.5)$ is noticeable. At the same time, the quadratic dependence $(f_{ab} = 1 + 2x - 2x^2)$ complicates the transition to multiflow ejector schemes, which have many outlet channels – three, four, or more. For this reason, when creating promising multiflow ejectors, we preferred the version of the nozzle apparatus with a square cross-section, where $(f_{ab} = 1)$. It should also be noted that the formation of a square or rectangular channel in the critical section of the nozzle opens prospects for the practical use of the Coanda effect, which may prove to be a decisive factor in the creation of a promising jet system.

To assess the energy efficiency of the round and square nozzles, we used the criterion (F_0/Q_0), with the initial temperature of the working gas being equal. To date, no significant differences have been found in this criterion. Based on the available data, a preliminary conclusion was made that the shape of the critical section does not affect the energy efficiency of the Laval nozzle. However, with the addition of data, this conclusion can be clarified. It should be noted that the experimental reversible Laval nozzle in our study has a square shape only in the critical section zone. A comprehensive consideration of the interrelated issues of thrust vector, trajectory planning, and control accuracy is planned for the subsequent stages of scientific research. These issues should be considered for UAV prototypes. At this stage of the research, a delta-wing UAV was selected as a prototype, the first numerical experiments were conducted for large angles of attack up to 90 °, and the prospects of the chosen direction of research were demonstrated (we plan to publish the results in subsequent articles).

The computer simulation findings allowed us to make a number of generalizations for the reversible nozzle apparatus option (Figures 3 to 7 and 13). In this example, the dependence of the mass flow rate on the working gas pressure can be represented as follows:

$$Q_0 = k_Q * P \tag{25}$$

where k_Q is an empirical coefficient reflecting the design features of the proposed nozzle apparatus; in the example under discussion, $k_Q = 0.0149\ [kg/(s * MPa)]$, for the range $(1.5\ MPa \leq P \leq 12\ MPa)$.

The dependence of thrust on the working gas pressure can be represented as follows:

$$F_0 = k_F * P + F_P \tag{26}$$

where k_F, F_P are empirical coefficient reflecting the design features of the proposed nozzle apparatus; in the example under discussion, $k_F = 29.371\ [N/MPa]$; $F_P = -14.338\ [N]$, for the range $(1.5\ MPa \leq P \leq 12\ MPa)$.

The wedge-shaped diaphragm allows for a linear relationship between the main parameters and the x coordinate in the interval $0 \leq x \leq 1$:

$$x = f_a = \frac{Q_a}{Q_0} = \frac{F_a}{F_0} \tag{27}$$

The developed mathematical model and Equations 25 to 27 allow for the transition to the creation of high-speed computational computer programs for modeling multiflow nozzle apparatuses (and multiflow ejectors, respectively), with thrust vector control within a full geometric sphere. In this case, to determine the values of the main parameters (for example, $Q_a;\ F_a$), no labor-intensive and time-consuming continuous modeling procedure (CFD) is required, with different values of the parameters $x; P$. The presented example of creating a mathematical model and a simple digital twin for a reversible nozzle apparatus shows good prospects for creating high-speed control systems (thrust vector control systems) applied to production technologies or high-speed and highly maneuverable transportation systems. The digital twin for a reversible nozzle apparatus can also be considered as part of a machine learning system, which reduces the dependence on continuous CFD modeling.

For laboratory testing of the operability of individual technical solutions, models and dummies of the nozzle apparatus were created using additive technologies. One of these dummies (developed in accordance with the scheme shown in Figure 9) is shown in Figure 30.

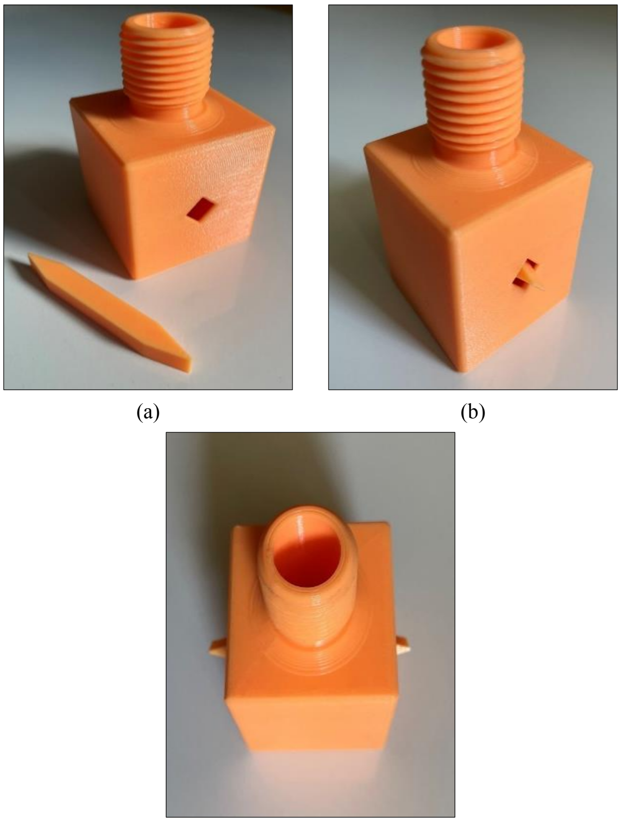

(a) (b)

(c)

Figure 30. Experimental two-flow nozzle apparatus dummy: a) housing and movable rod with two wedge-shaped diaphragms; b) nozzle apparatus after assembly; c) nozzle apparatus after assembly (top view)

With the transition to the widespread practical use of metal powders, cutting-edge additive technologies will open up new possibilities in jet and reactive technology when working with nozzle apparatuses and flow channels. Some of the results of the completed studies will be used for training modern designers and for further development of the Euler methodology. The digital twin for a reversible nozzle apparatus presented in this article and formulas (25-27) allow observing changes in operating parameters when scaling the product within the framework of computer CFD modeling. No special or novel gas-dynamic effects have been observed with such scaling. However, the use of additive technologies in the manufacture of models for testing individual technical solutions, including the study of known problems associated with scaling, is envisaged.

4.2. Discussion of Typical Schemes for Thrust Vector Control

Regarding the prepared scientific groundwork [4-7], Figure 31 schematically shows the basic operating modes (options) for a jet unit designed to control the thrust vector within a full geometric sphere. The arrows in the diagrams in Figure 31 indicate the flow direction. The possibility of controlling flows with high and low energy densities at high and low temperatures of the fluid medium is demonstrated. The possibility of controlling hot high-speed flows by influencing cold flows in the ejector channels was demonstrated, thereby removing the control system from the zone of high temperatures and high velocities in the flows. The materials presented in Figures 10-24 reflect the capabilities of thrust vector control according to schemes H3, H4 and H5 in Figure 31; at the same time, on this basis, all options from Figure 31 will be considered when continuing the research.

In the course of continuing research, new schemes (for thrust vector control) will supplement the contents shown in Figure 31. In combination with previously published materials [4-7], the data in Figure 31 form the information base for the development of scientific and design work aimed at solving complex problems of thrust vector control under extreme conditions within the full geometric sphere. Moreover, within the full geometric sphere, the thrust vector is regulated by the module, direction, and changes in the starting point coordinates. This opens new opportunities for controlling the six degrees of freedom of aircraft, including options with Euler angles. The presented jet systems allow for the creation of pitch, roll, and yaw moments. Scientific developments are also aimed at creating high-velocity and extremely maneuverable unmanned vehicles for operation in air, sea, and land when solving various scientific and practical problems.

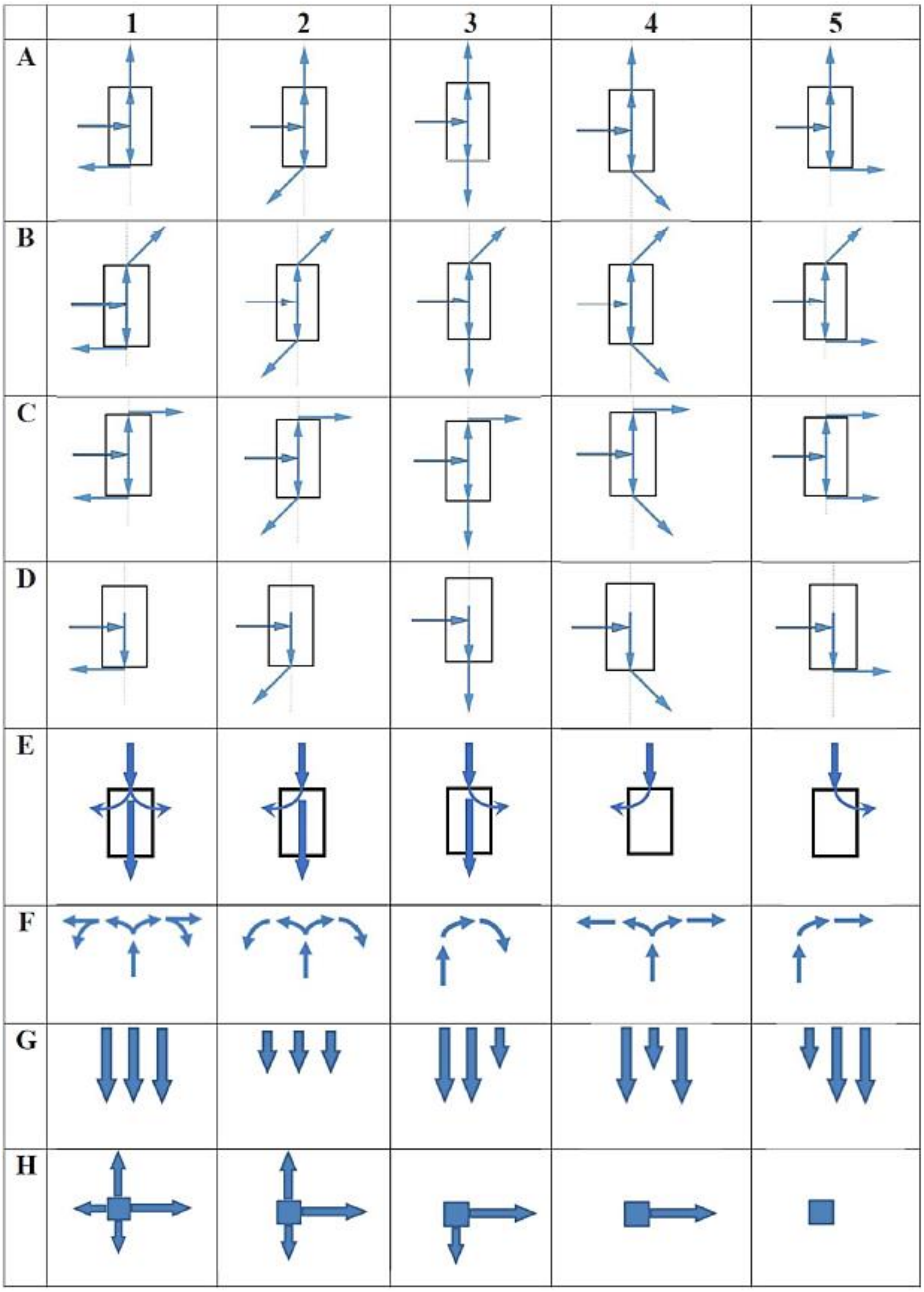

Figure 31. Operating modes of the nozzle apparatus (jet unit)

4.3. Discussion of Issues on the Development of the Theory of Solving Scientific, Inventive and Design Problems

For educational purposes, in modern conditions with big data, it is advisable to create a new (digital) format for presenting the Euler methodology. The question of the characteristics of a good scientific theory is very important, and among the set of usual answers, Kuhn in Pirozelli [58] chose the following five answers:

- The theory should be accurate (in agreement with the results of previous experiments and observations).
- The theory should be consistent (with itself and other accepted theories applicable to similar areas of nature).
- The theory should have a wide scope of application.
- The theory should be simple.
- This theory should be fruitful in opening new research horizons. It should reveal new phenomena that previously remained unnoticed among already known phenomena, and (the theory) should consider the individual characteristics of scientists (and students).

The “trial and error method” should not be rejected, since we all learn from our mistakes [10]. The solution of almost any optimization problem presupposes the presence of several options for solving the problem; however, ultimately, one solution, the best one, is chosen. The remaining options are thrown into the same basket where all erroneous solutions are stored (located). In addition, experts note that for training artificial intelligence, it is important to use all possible options for solving a specific problem, rather than one final best option that makes it light and is recognized as useful in the scientific community, and even more so in a scientific journal. Based on the philosophy of technology, any kind of development or evolution is inherently associated with the practical implementation of the “trial and error method.”

According to Euler (formulas 1-3), big data can be considered an expanding knowledge base [4-7]. From a fundamental science standpoint, this knowledge base is constantly expanding its list of possibilities. This refers to the possibility of practical use of this knowledge in real competition among people. However, a question remains: Has a specific person used this knowledge? From the standpoint of applied science, applied research aims at the practical implementation of opportunities to win in competition. Whoever has more Knowledge that people have more opportunities to win [59]. So far, there are no people with knowledge since birth, and everything must be persistently studied. To train modern designers according to the Euler methodology, it is necessary to use CFD technologies, in particular, and use the digital format in general.

Hypotheses are developed within the framework of multiparameter (multidimensional) problems, using ideas and the Euler methodology, with the prospect of more active practical applications of artificial intelligence tools. The basic direction of research is to study the processes of fluid flow interaction with a solid wall when controlling the thrust vector in extreme conditions, with the discovery of new opportunities to go beyond known boundaries while expanding the field of knowledge. Within the framework of fundamental research, the goal is to expand the list of opportunities to obtain competitive advantage in the development of science and technology. Within the framework of applied research, the goal was to develop recommendations for the practical use of new competitive advantages based on the above list of opportunities. According to the Euler methodology, modern scientific, inventive, and design problems should be considered in a single complex as part of interdisciplinary research, including the tools of the philosophy of technology and the modern digital system MSIF. The comprehensive discipline of multi-source information fusion (MSIF) with interdisciplinary innovative potential allows the integration of information to create a common accurate description that can help in effective decision-making and forecasting [16], including the use of artificial intelligence. In such interdisciplinary studies, mathematics and computer technologies (CFD) act as the connecting links.

Within the framework of the MSIF system, it should be noted that when searching for the causes of any phenomenon in general, according to the teachings of Aristotle, it is necessary to ask four questions, the answers to which will allow us to obtain a complete understanding of the subject being studied [56].

- The question of the material cause. What material is the subject made?
- The question of the formal cause. What form does the subject have?
- The question of the final cause (goal). For what purpose does the subject exist?
- The question of the cause of production. By which action was the subject produced?

The subject being studied can be of natural or artificial origin (as a result of the work of a person or specialist). Descartes noted that all known sciences borrowed their principles from philosophy [9]. Recalling Aristotle, it can be emphasized that the efforts to think through early themes of thought even more deeply are not a foolish desire to update the past but a sober readiness to be surprised by the future character of the early [56]. At present, rereading Aristotle, Descartes, and Euler within the framework of the advanced digital system MSIF, the first question regarding the material cause should be associated with the selection of structural materials and with the implementation of strength analysis within computer modeling technologies (CFD). The second question regarding the formal cause today is associated with the creation of a computer three-dimensional solid model (or a digital twin of CFD), indicating all relevant geometric parameters that make it possible to describe the geometric shape of the object under study. Currently, the third question about the final cause (about the goal) is more often associated with solving a CFD optimization problem to gain competitive advantages over known scientific and technical developments (within the framework of improving gas-dynamic or hydrodynamic processes that lead to a certain advantage or economic benefit compared to a competitor or opponent). The fourth question regarding the cause of production has undergone some changes today, and new options appear in the description of the performer who acts and produces the studied object. Instead of a person, a human-machine system or artificial intelligence can act. The mathematical model according to Euler (formulas 1-3) includes four groups of parameters with indices [4-7], that correspond to the four questions of Aristotle: indices (a, b, c, d) for the corresponding parameters $(x_{ai};\ x_{bi};\ x_{ci};\ x_{di})$.

René Descartes wrote that he never considered his mind to be more perfect than others, and he often wished to have such a quick thought, such a clear and distinct imagination, or such an extensive and reliable memory as some others [9]. Today, within the framework of the modern digital system MSIF, René Descartes' wish to have such a quick, extensive, and reliable memory has been fully fulfilled. Currently, CFD computer technologies are available to humans for quickly solving the most complex problems and memorizing (using) large amounts of information. In this regard, the potential capabilities of artificial intelligence are still difficult to assess, but it is clear that these capabilities are constantly increasing, and a human-machine system can take place in the broadest sense of the word (term), as interpreted in the field of philosophy of technology. It seems that competitive struggle (in all spheres of life) intensifies with the strengthening of artificial intelligence. Under such conditions, old truths [58-60] require even more attention and new and more thoughtful reading.

The accuracy of CFD computer simulations requires large computational resources and time, particularly when considering complex geometric shapes [61, 62]. Machine learning is now considered an additional research direction because of its ability to learn from data and make predictions based on these data. Using machine learning algorithms, it is possible to reduce the dependence on continuous CFD simulation [63], including when solving particularly complex problems in control systems for a group (swarm) of UAVs [64-66].

The digital twin for the reversible nozzle apparatus presented in this article and Equations 25 to 27 can be considered as a promising fragment for the corresponding machine learning system, which will reduce the dependence on continuous CFD simulation when creating control systems for complex products or for groups of computerized autonomous objects.

5. Conclusions

5.1. Scientific Novelty of the Development

New versions of multiflow nozzle apparatus equipped with wedge-shaped movable inserts that allow for the distribution of high-density energy between the working chambers of a multiflow ejector with thrust vector control within a full geometric sphere were developed and prepared for patenting. The formulated hypothesis on the possibility of creating a universal and simple control system for a multiflow nozzle with thrust-vector control within a full geometric sphere was partially confirmed.

5.2. Theoretical Contributions

New methodological approaches have been proposed for designing complex jet systems with thrust cutoff (tailoff) capabilities, while maintaining the nominal operating mode of the working gas source.

5.3. Practical Significance

Practical recommendations and new capabilities for extreme thrust vector control within a full geometric sphere with the coordinated operation of controlled nozzle apparatuses and a group of several working gas sources were proposed. The research results can be used in the power engineering sector and unmanned and autonomous vehicles for various purposes (land, sea, and air). An area for the development of the Euler methodology is proposed, as applied to practical problems in higher education, in the training of modern designers.

5.4. Limitations and Future Research

The use of artificial intelligence to solve scientific and inventive problems with many parameters remains a large and unsolved problem. Future research in the field of thrust-vector jet control systems will be aimed at a comprehensive consideration of the problems of six degrees of freedom in a three-dimensional space regarding Euler angles. A scientific groundwork was prepared to consider the problems of flight path planning (for example, for an unmanned aerial vehicle) regarding new possibilities for extreme maneuvering that are not yet available for known aircraft designs.

6. Declarations

6.1. Author Contributions

Conceptualization, Y.A.S.; methodology, M.A.M.; software, E.I.K.; validation K.A.T.; formal analysis, V.V.V.; investigation, K.A.T.; resources, Y.A.S.; data curation, A.V.B.; writing—original draft preparation, K.A.T., E.I.K., V.V.V., and A.V.B.; writing—review and editing, Y.A.S. and M.A.M.; visualization, E.I.K.; supervision, M.A.M.; project administration, M.A.M.; funding acquisition, Y.A.S. All authors have read and agreed to the published version of the manuscript.

6.2. Data Availability Statement

The data presented in this study are available on request from the corresponding author.

6.3. Funding

The research was financially supported by the Russian Ministry of Education and Science within the framework of the government task in scientific activity, subject number FSZE-2023-0004.

6.4. Conflicts of Interest

The authors declare no conflict of interest.

7. References

[1] Xu, Z., Liu, B., Tong, Y., Dong, Z., & Feng, Y. (2024). Modeling and Control of Ejector-Based Hydrogen Circulation System for Proton Exchange Membrane Fuel Cell Systems. Energies, 17(11), 2460. doi:10.3390/en17112460.

[2] Li, J., Wu, T., Cheng, C., Li, J., & Zhou, K. (2024). A Review of the Research Progress and Application of Key Components in the Hydrogen Fuel Cell System. Processes, 12(2), 249. doi:10.3390/pr12020249.

[3] Kim, S. W. (2024). Thrust Augmenter. Japanese Patent, JP2024516044, Patent Attorney Corporation Haruka International Patent Office, Tokyo, Japan. Available online: https://www.freepatentsonline.com/JP2024516044.html (accessed on October 2024). (In Japanese).

[4] Sazonov, Y. A., Mokhov, M. A., Gryaznova, I. V., Voronova, V. V., Tumanyan, K. A., & Konyushkov, E. I. (2023). Thrust Vector Control within a Geometric Sphere, and the Use of Euler's Tips to Create Jet Technology. Civil Engineering Journal (Iran), 9(10), 2516–2534. doi:10.28991/CEJ-2023-09-10-011.

[5] Sazonov, Y. A., Mokhov, M. A., Gryaznova, I. V., Voronova, V. V., Tumanyan, K. A., & Konyushkov, E. I. (2023). Solving Innovative Problems of Thrust Vector Control Based on Euler's Scientific Legacy. Civil Engineering Journal (Iran), 9(11), 2868–2895. doi:10.28991/CEJ-2023-09-11-017.

[6] Sazonov, Y. A., Mokhov, M. A., Gryaznova, I. V., Voronova, V. V., Tumanyan, K. A., & Konyushkov, E. I. (2023). Methods for Regulating Ejector Systems Within Interdisciplinary Research Using Computer Modeling. International Journal on Technical and Physical Problems of Engineering, 15(4), 306–320.

[7] Sazonov, Y. A., Mokhov, M. A., Bondarenko, A. V., Voronova, V. V., Tumanyan, K. A., & Konyushkov, E. I. (2023). Interdisciplinary Studies of Jet Systems using Euler Methodology and Computational Fluid Dynamics Technologies. HighTech and Innovation Journal, 4(4), 703–719. doi:10.28991/HIJ-2023-04-04-01.

[8] Qian, D., & Lawal, A. (2006). Numerical study on gas and liquid slugs for Taylor flow in a T-junction microchannel. Chemical Engineering Science, 61(23), 7609-7625. doi:10.1016/j.ces.2006.08.073.

[9] Descartes, R. (1878). Discourse on the Method of Rightly Conducting one's Reason and Seeking Truth in the Sciences (Vol. 1). Hachette et Cie, Paris, France. (In Russian).

[10] Popper, K. (2002) Conjectures and Refutations: The Growth of Scientific Knowledge. Routledge, Milton Park, United Kingdom.

[11] Fernandes, G., & Maldonado, V. (2024). The U.S. Air Force Next-Generation Air-Refueling System: A Resurgence of the Blended Wing Body? Aerospace, 11(6), 494. doi:10.3390/aerospace11060494.

[12] Xu, S., Liu, Y., Zhang, J., & Zheng, Y. (2024). Preliminary Design and Optimization of Primary Structures for a Tilt-Duct UAV. Aerospace, 11(4), 286. doi:10.3390/aerospace11040286.

[13] Vankan, W. J., Lammen, W. F., Scheers, E., Dewitte, P. J., & Defoort, S. (2024). Concept Evaluation of Radical Short–Medium-Range Aircraft with Turbo-Electric Propulsion. Aerospace, 11(6), 477. doi:10.3390/aerospace11060477.

[14] Wang, J., Zhang, X., Lu, J., & Tang, Z. (2024). Numerical Simulation and Experimental Study on the Aerodynamics of Propulsive Wing for a Novel Electric Vertical Take-Off and Landing Aircraft. Aerospace, 11(6), 431. doi:10.3390/aerospace11060431.

[15] Xia, J., & Zhou, Z. (2024). The Modeling and Control of a Distributed-Vector-Propulsion UAV with Aero-Propulsion Coupling Effect. Aerospace, 11(4), 284. doi:10.3390/aerospace11040284.

[16] Li, X., Dunkin, F., & Dezert, J. (2024). Multi-source information fusion: Progress and future. Chinese Journal of Aeronautics, 37(7), 24–58. doi:10.1016/j.cja.2023.12.009.

[17] Wang, Z., Gong, H., Nie, M., & Liu, X. (2024). Research on Multi-UAV Cooperative Dynamic Path Planning Algorithm Based on Conflict Search. Drones, 8(6), 274. doi:10.3390/drones8060274.

[18] Fang, Z., & Savkin, A. V. (2024). Strategies for Optimized UAV Surveillance in Various Tasks and Scenarios: A Review. Drones, 8(5), 193. doi:10.3390/drones8050193.

[19] Meng, Q., Chen, K., & Qu, Q. (2024). PPSwarm: Multi-UAV Path Planning Based on Hybrid PSO in Complex Scenarios. Drones, 8(5), 192. doi:10.3390/drones8050192.

[20] Sun, T., Sun, W., Sun, C., & He, R. (2024). Multi-UAV Formation Path Planning Based on Compensation Look-Ahead Algorithm. Drones, 8(6), 251. doi:10.3390/drones8060251.

[21] Sieber, C., Vieira da Silva, L. M., Grünhagen, K., & Fay, A. (2024). Rule-Based Verification of Autonomous Unmanned Aerial Vehicles. Drones, 8(1), 26. doi:10.3390/drones8010026.

[22] Barakou, S. C., Tzafestas, C. S., & Valavanis, K. P. (2024). A Review of Real-Time Implementable Cooperative Aerial Manipulation Systems. Drones, 8(5), 196. doi:10.3390/drones8050196.

[23] Gómez Arnaldo, C., Zamarreño Suárez, M., Pérez Moreno, F., & Delgado-Aguilera Jurado, R. (2024). Path Planning for Unmanned Aerial Vehicles in Complex Environments. Drones, 8(7), 288. doi:10.3390/drones8070288.

[24] Huang, G., Hu, M., Yang, X., Wang, X., Wang, Y., & Huang, F. (2024). A Review of Constrained Multi-Objective Evolutionary Algorithm-Based Unmanned Aerial Vehicle Mission Planning: Key Techniques and Challenges. Drones, 8(7), 316. doi:10.3390/drones8070316.

[25] Aben, E., Yussupova, S., Akhmetkanov, D., Yelzhanov, E., & Sarybayev, N. (2024). Research into Uranium Characteristics and Content in a Pregnant Solution During Leaching with Oxygen Saturation. Civil Engineering Journal (Iran), 10(5), 1606–1615. doi:10.28991/CEJ-2024-010-05-016.

[26] Bu, Y., Yan, Y., & Yang, Y. (2024). Advancement Challenges in UAV Swarm Formation Control: A Comprehensive Review. Drones, 8(7), 320. doi:10.3390/drones8070320.

[27] Yu, H., Yang, X., Zhang, Y., & Jiang, Z. (2024). Cooperative Target Fencing Control for Unmanned Aerial Vehicle Swarm with Collision, Obstacle Avoidance, and Connectivity Maintenance. Drones, 8(7), 317. doi:10.3390/drones8070317.

[28] Ligotskiy, D. N., & Argimbaeva, K. V. (2024). The sectional formation technology of an anthropogenic deposit with its subsequent mining using a hydraulic pull shovel. Sustainable Development of Mountain Territories, 16(1), 111–121. doi:10.21177/1998-4502-2024-16-1-111-121.

[29] Gil, J. (2023). Modular unmanned aerial vehicle system for adaptable parcel delivery. US Patent 11,794,931 B2, United States Patent, Alexandria, United States. Available online: https://www.freepatentsonline.com/11794931.pdf (accessed on October 2024).

[30] Carmack, S G., Narasimha R. L., & Nima S. M. (2017). Using multirotor lifters to deploy fixed wing aircraft. US Patent 9,630,712 B1, United States Patent, Alexandria, United States. Available online: https://www.freepatentsonline.com/9630712.pdf (accessed on October 2024).

[31] Bosma, M. B. (2023). Helicopter winch cable stabilizer. US Patent 11,618,584 B2, United States Patent, Alexandria, United States. Available online: https://www.freepatentsonline.com/11618584.pdf (accessed on October 2024).

[32] Yılmazer, C., & Arı Güner, H. A. (2024). Physical and Numerical Modeling of Flow in a Meandering Channel. Water (Switzerland), 16(11), 1547. doi:10.3390/w16111547.

[33] Famellos, P., Skevas, A., Koutsiadis, A., Koutsouras, C., & Panagiotou, P. (2024). Design and Analysis of a Base Bleed Unit for the Drag Reduction of a High-Power Rocket Operating at Transonic Speeds. Aerospace, 11(5), 385. doi:10.3390/aerospace11050385.

[34] Papadakis, N., & Condaxakis, C. (2024). An Experimental Performance Assessment of a Passively Controlled Wind Turbine Blade Concept: Part B—Material Oriented with Glass-Fiber-Reinforced Polymer. Energies, 17(13), 3286. doi:10.3390/en17133286.

[35] Koca, K., & Genç, M. S. (2024). Role of Partial Flexibility on Flow Evolution and Aerodynamic Power Efficiency over a Turbine Blade Airfoil. Aerospace, 11(7), 571. doi:10.3390/aerospace11070571.

[36] Meng, Q., Hu, Y., Wei, W., Yao, Z., Ke, Z., Zhang, H., Zhao, M., & Yan, Q. (2024). Aerodynamic Hinge Moment Characteristics of Pitch-Regulated Mechanism for Mars Rotorcraft: Investigation and Experiments. Drones, 8(7), 277. doi:10.3390/drones8070277.

[37] Dong, W., Wang, X., Lin, Q., Cheng, C., & Zhu, L. (2024). A Weighted Feature Fusion Model for Unsteady Aerodynamic Modeling at High Angles of Attack. Aerospace, 11(5), 339. doi:10.3390/aerospace11050339.

[38] Farì, S., Sagliano, M., Macés Hernández, J. A., Schneider, A., Heidecker, A., Schlotterer, M., & Woicke, S. (2024). Physical Modeling and Simulation of Reusable Rockets for GNC Verification and Validation. Aerospace, 11(5), 337. doi:10.3390/aerospace11050337.

[39] Wu, Q., & Ren, Q. (2024). Tuning the Ballistic Performance of a Single-Burning-Rate Grain Solid Rocket Motor via New Discontinuous Embedded Metal Wires. Aerospace, 11(4), 308. doi:10.3390/aerospace11040308.

[40] Georgievich, D. G., Sergeevich, K. A., Fedorovich, V. V., & Yurevich, S. Y. (2018). Thrust cut-off assembly of solid-propellant rocket engine. RF Patent RU 2 664 638 C2, Russian Federation, Moscow, Russia. Available online: https://www.fips.ru/ofpstorage/Doc/IZPM/RUNWC1/000/000/002/664/638/ИЗ-02664638-00001/document.pdf (accessed on October 2024). (In Russian).

[41] Permitin, A. V., & Pavel A. S. (2019). Solid rocket engine cutout assembly. RF Patent RU 2 691 002 C1, Russian Federation, Moscow, Russia. Available online: https://www.fips.ru/ofpstorage/Doc/IZPM/RUNWC1/000/000/002/691/002/ИЗ-02691002-00001/document.pdf (accessed on October 2024). (In Russian).

[42] Arkhipov, V. A., Sergej, S. B., Aleksandr, B. V., Aleksandr S. Z., Boris, V. P., & Lilija, A. S. (2014). Hybrid rocket engine. RF Patent RU 2 569 960 C1, Russian Federation, Moscow, Russia. Available online: https://new.fips.ru/Archive/PAT/2015FULL/2015.12.10/DOC/RUNWC1/000/000/002/569/960/DOCUMENT.PDF (accessed on October 2024). (In Russian).

[43] Yun, M. S., Roh, T. S., & Lee, H. J. (2024). Analysis of Development Trends for Rotating Detonation Engines Based on Experimental Studies. Aerospace, 11(7), 570. doi:10.3390/aerospace11070570.

[44] Shao, S., Yue, S., Qiao, H., Liu, P., & Ao, W. (2024). Numerical and Experimental Analyses of the Effect of Water Injection on Combustion of Mg-Based Hydroreactive Fuels. Aerospace, 11(7), 542. doi:10.3390/aerospace11070542.

[45] Techavijit, P., Sukchalerm, P., Wongphuangfuthaworn, N., & Kiyapaet, S. (2024). Fly-around-the-World Near-Space Picosatellite for Cost-Effective School Space Projects. Aerospace, 11(7), 557. doi:10.3390/aerospace11070557.

[46] Caballero-Martin, D., Lopez-Guede, J. M., Estevez, J., & Graña, M. (2024). Artificial Intelligence Applied to Drone Control: A State of the Art. Drones, 8(7), 296. doi:10.3390/drones8070296.

[47] Wang, H., Zhou, D., Zhang, Y., & Lou, C. (2024). Compound Control Design of Near-Space Hypersonic Vehicle Based on a Time-Varying Linear Quadratic Regulator and Sliding Mode Method. Aerospace, 11(7), 567. doi:10.3390/aerospace11070567.

[48] Ren, Y., Zhu, F., Sui, S., Yi, Z., & Chen, K. (2024). Enhancing Quadrotor Control Robustness with Multi-Proportional–Integral–Derivative Self-Attention-Guided Deep Reinforcement Learning. Drones, 8(7), 315. doi:10.3390/drones8070315.

[49] Kindström Andersson, K., & Andersson, K. E. (2024). Development of Scenarios as Problem-Space Descriptions in Aerospace Conceptual Design. Aerospace, 11(7), 565. doi:10.3390/aerospace11070565.

[50] Tyapkin, V. N., Korovin, A. V., Nerovny, V. V., Ishchuk, I. N., & Kabulova, E. G. (2018). Precision characteristics of the ground-based user equipment of satellite radio navigation system employing pseudolites in noisy environments. International Review of Aerospace Engineering, 11(2), 58–65. doi:10.15866/irease.v11i2.13938.

[51] Xi, A., & Cai, Y. (2024). Deep Reinforcement Learning-Based Differential Game Guidance Law against Maneuvering Evaders. Aerospace, 11(7), 558. doi:10.3390/aerospace11070558.

[52] Cao, W., Huang, J., & Chang, S. (2024). Data-Driven-Method-Based Guidance Law for Impact Time and Angle Constraints. Aerospace, 11(7), 540. doi:10.3390/aerospace11070540.

[53] Xie, Z., Wei, C., Cui, N., & Guan, Y. (2024). An Analytical Reentry Solution Based Online Time-Coordinated A* Path Planning Method for Hypersonic Gliding Vehicles Considering No-Fly-Zone Constraint. Aerospace, 11(6), 499. doi:10.3390/aerospace11060499.

[54] Ansoff, H. I., Kipley, D., Lewis, A. O., Helm-Stevens, R., & Ansoff, R. (2019). Implanting Strategic Management. Springer International Publishing, Cham, Switzerland. doi:10.1007/978-3-319-99599-1.

[55] Yachmenova, L. A., Syrkov, A. G., & Kabirov, V. R. (2023). Features of obtaining surface-modified metals with minimal carbon footprint. Non-Ferrous Metals, 55(2), 33–40. doi:10.17580/nfm.2023.02.06.

[56] Heidegger, M. (1954). The question of technology. Vorträge und Aufsätze, 5, 9-40. (In German)

[57] Sokolov, E.Y., & Zinger, N. M. (1989). Jet units (3rd Ed.). Energiya, Moscow, Russia. (in Russian).

[58] Pirozelli, P. (2019). Thomas Kuhn’s theory of rationality. Manuscrito, 42(3), 1–46. doi:10.1590/0100-6045.2019.V42N3.PP.

[59] Sun, T. (2024). The Art of War. Available online: https://classics.mit.edu/Tzu/artwar.html (accessed on October 2024).

[60] Hübner, K. (1983). The Critique of Scientific Reason. University of Chicago Press, Chicago, United States.

[61] Zhou, J., Zhang, H., Hua, M., Wang, F., & Yi, J. (2024). P-DRL: A Framework for Multi-UAVs Dynamic Formation Control under Operational Uncertainty and Unknown Environment. Drones, 8(9), 475. doi:10.3390/drones8090475.

[62] Wei, S.-S., Li, M.-C., Lai, A., Chou, T.-H., & Wu, J.-S. (2024). A Review of Recent Developments in Hybrid Rocket Propulsion and Its Applications. Aerospace, 11(9), 739. doi:10.3390/aerospace11090739.

[63] Sánchez Muñoz, J. A., Lagarza-Cortés, C., & Ramírez-Cruz, J. (2024). Aerodynamic Drag Coefficient Prediction of a Spike Blunt Body Based on K-Nearest Neighbors. Aerospace, 11(9), 757. doi:10.3390/aerospace11090757.

[64] Zhao, Z., Wan, Y., & Chen, Y. (2024). Deep Reinforcement Learning-Driven Collaborative Rounding-Up for Multiple Unmanned Aerial Vehicles in Obstacle Environments. Drones, 8(9), 464. doi:10.3390/drones8090464.

[65] Zhao, L., Chen, B., & Hu, F. (2024). Research on Cooperative Obstacle Avoidance Decision Making of Unmanned Aerial Vehicle Swarms in Complex Environments under End-Edge-Cloud Collaboration Model. Drones, 8(9), 461. doi:10.3390/drones8090461.

[66] Abu Salem, K. (2024). The Key Role of Research in Flight Dynamics, Control, and Simulation for Advancing Aeronautical Sciences. Aerospace, 11(9), 734. doi:10.3390/aerospace11090734.